



HAL
open science

Sol-gel synthesis of collagen-inspired peptide hydrogel

Cécile Echalié, Said Jebors, Guillaume Laconde, Luc Brunel, Pascal Verdié, Léa Causse, Audrey Bethry, Baptiste Legrand, Hélène van den Berghe, Xavier Garric, et al.

► To cite this version:

Cécile Echalié, Said Jebors, Guillaume Laconde, Luc Brunel, Pascal Verdié, et al.. Sol-gel synthesis of collagen-inspired peptide hydrogel. *Materials Today*, 2017, 20 (2), pp.59-66. 10.1016/j.mattod.2017.02.001 . hal-01516237

HAL Id: hal-01516237

<https://hal.science/hal-01516237v1>

Submitted on 4 May 2017

HAL is a multi-disciplinary open access archive for the deposit and dissemination of scientific research documents, whether they are published or not. The documents may come from teaching and research institutions in France or abroad, or from public or private research centers.

L'archive ouverte pluridisciplinaire **HAL**, est destinée au dépôt et à la diffusion de documents scientifiques de niveau recherche, publiés ou non, émanant des établissements d'enseignement et de recherche français ou étrangers, des laboratoires publics ou privés.

Public Domain

Sol-gel synthesis of collagen-inspired peptide hydrogel

Cécile Echalié^{1,2}, Said Jebors¹, Guillaume Laconde¹, Luc Brunel¹, Pascal Verdié¹, Léa Causse¹, Audrey Bethry¹, Baptiste Legrand¹, Hélène Van Den Berghe¹, Xavier Garric¹, Danièle Noël³, Jean Martinez¹, Ahmad Mehdi², Gilles Subra¹

¹Institut des Biomolécules Max Mousseron (IBMM), UMR5247 Université de Montpellier, CNRS, ENSCM, France.

²Institut Charles Gerhardt de Montpellier (ICGM), UMR5253 Université de Montpellier, CNRS, ENSCM, France.

³Institute for Regenerative Medicine and Biotherapy (IRMB), Inserm U1183, CHU, Université de Montpellier, France.

Corresponding author: gilles.subra@umontpellier.fr

Conceiving biomaterials able to mimic the specific environments of extracellular matrices are a prerequisite for tissue engineering applications. Numerous types of polymers (PEG, PLA, etc.) have been used for the design of biocompatible scaffolds, but they are still less efficient than natural biopolymers such as collagen extracts. Chemically modified and loaded with different bioactive factors, biopolymers afford an environment favourable to cell proliferation and differentiation. Unfortunately, they present several drawbacks, such as weak batch-to-batch reproducibility, potential immunogenicity and high cost of production. Herein we propose a fully synthetic covalent hydrogel obtained by sol-gel polymerisation of a silylated peptide. We selected a short and low molecular building-block derived from the consensus collagen sequence [Pro-Hyp-Gly]. Interestingly, the sol-gel process occurs in physiological buffer, enabling the embedment of stem cells. This collagen-inspired hydrogel provides a cell-friendly environment comparable to natural collagen substrates, demonstrating its potency as a biomimetic scaffold.

1. Introduction

Hydrogels are exceptional biomaterials, especially for their use as scaffolds for tissue engineering and as matrices for drug and gene delivery. Depending on the type of bonds that are formed during their fabrication process, physical or chemical hydrogels can be obtained. Physical hydrogels are reversible, due to the weak interactions involved in the biomaterial (e.g. hydrogen and ionic bonds), and are attractive as injectable materials due to their shear thinning (or thixotropic behavior). On the other hand, chemical hydrogels cross-linked by covalent bonds, are more stable and thus suitable for a wider range of applications including cell culture. A large family of them is based on synthetic polymers such as poly(lactic-co-glycolic acid) PLGA,[1] polyacrylamides,[2,3] polyhydroxyethylmethacrylate (PHEMA)[4] or polyethyleneglycol (PEG)[5]. However all these materials fail to mimic the complexity of natural tissues and have to be further functionalized with peptide ligands derived from extracellular matrix (ECM) proteins (e.g. fibronectin, laminin) for efficient cell adhesion.[6,7]

To improve the resemblance with natural tissues, it is also possible to form a hydrogel by covalently linking chemically-modified synthetic polymers [i.e. poly(N-isopropylacrylamide) (NIPAM), PEG, etc.] with chemically-modified natural biopolymers [i.e. polysaccharides, heparin, etc.]. For example, hydrazide-modified NIPAM was reacted with aldehyde-modified carboxymethyl cellulose, to yield injectable hydrogels.[8] A starPEG-heparin hydrogel was obtained after chemical modification of both starPEG and heparin with a maleimide (via carbodiimide/active ester) [9], which can be cross-linked with the thiol side-chains of a cysteine-containing peptide by Michael addition.[10][11] A analogue method was used to

cross-link thiol-modified gelatin and hyaluronic acid with PEG bis-acrylate.[12] Among the described conjugation methods that have been employed for polymer cross-linking, the embedment of cells drastically restrains the choice to non-toxic reagents, and to the absence of side-products coming from the reticulation reaction (i.e. active esters, metals, etc.).

Hydrogels obtained directly from cross-linked natural biopolymers are more adapted to cell survival and proliferation. Photopolymerization of methacrylated gelatin[13], chitosan[14] and hyaluronic acid[15] were used to prepare hydrogels. Nevertheless, these natural polymers are usually costly, they encounter low batch-to-batch reproducibility, microbial contaminants during the isolation process and potential immunogenicity in the case of animal extracts.

In this context, we propose a novel type of biomaterial, combining the biocompatibility of natural polymers, with the ease of synthesis and modification afforded by synthetic molecules. We defined four requirements to address the problems raised by existing materials.

(i) The starting materials should be synthetic to avoid purification problems encountered with extraction of natural biopolymers, and to facilitate the scale-up of the synthesis; (ii) The formation of the hydrogel network should be compatible with the inclusion of cells, avoiding the use of any chemical reagent; (iii) The process should be modular and should allow the covalent incorporation of any bioactive moiety in one single step; (iv) The resulting hydrogels should favour cell adhesion and proliferation, without the need of further addition of adhesion ligands.

These challenges were tackled by the design and synthesis of a bis-silylated low molecular building block (1612 g/mol) able to undergo sol-gel process, through hydrolysis and condensation in a biological buffer, yielding a three-dimensional network (Figure 1 A). We have already reported the synthesis of bioactive PEG-based chemical hydrogels by this type of soft chemistry route[16]. In this study, we substituted the biologically inert PEG by a peptide to give inherent cell-friendly properties to the network.

Considering the significance of collagen in tissue engineering[17], extensive work has been performed to mimic its multi-hierarchical structure with synthetic peptides. Among the general repetitive triplet motifs X-Y-Gly, the Pro-Hyp-Gly tripeptide is one of the most common stabilizing sequence found in collagens.[18] Very short oligopeptides based on this sequence were shown to adopt a polyproline II (PPII) helix conformation.[19] In natural collagen, three peptide sequences adopting a PPII structure wrap around each other to form a right-handed supercoil triple helix. It has been established that a minimal oligopeptide length is required to get stable triple helix structure. This latter structure was generally observed using nine or more X-Y-Gly triplets.[20–23] Moreover, to stabilize the self-assembly of synthetic collagen peptides, several strategies have been developed such as disulphide bridges formation,[24] ionic interactions between anionic and cationic side chains,[26,27] and hydrogen bond networks.[28]

In contrast with the ongoing research related to the design of peptide-based collagen mimics, we did not aim at reproducing the supramolecular structure of natural collagen. We focussed on the multiple presentation of Pro-Hyp-Gly motif, structured in PPII conformation, within a tri-dimensional matrix. We hypothesise that such artificial but collagen-inspired matrix could advantageously replace polymers to form hydrogels favouring cell culture with an efficiency comparable to that of collagen-based materials. We selected the peptide sequence (Pro-Hyp-Gly)₃ whose size was too small to expect the formation of triple helix, but long enough to adopt a well-defined PPII structure.[19] At last, the collagen-inspired sequence was flanked by two lysine residues and triethoxysilane groups were introduced on the lysine side-chains

using a flexible linker. Silyl moieties are the anchoring points promoting the covalent assembly of the network.

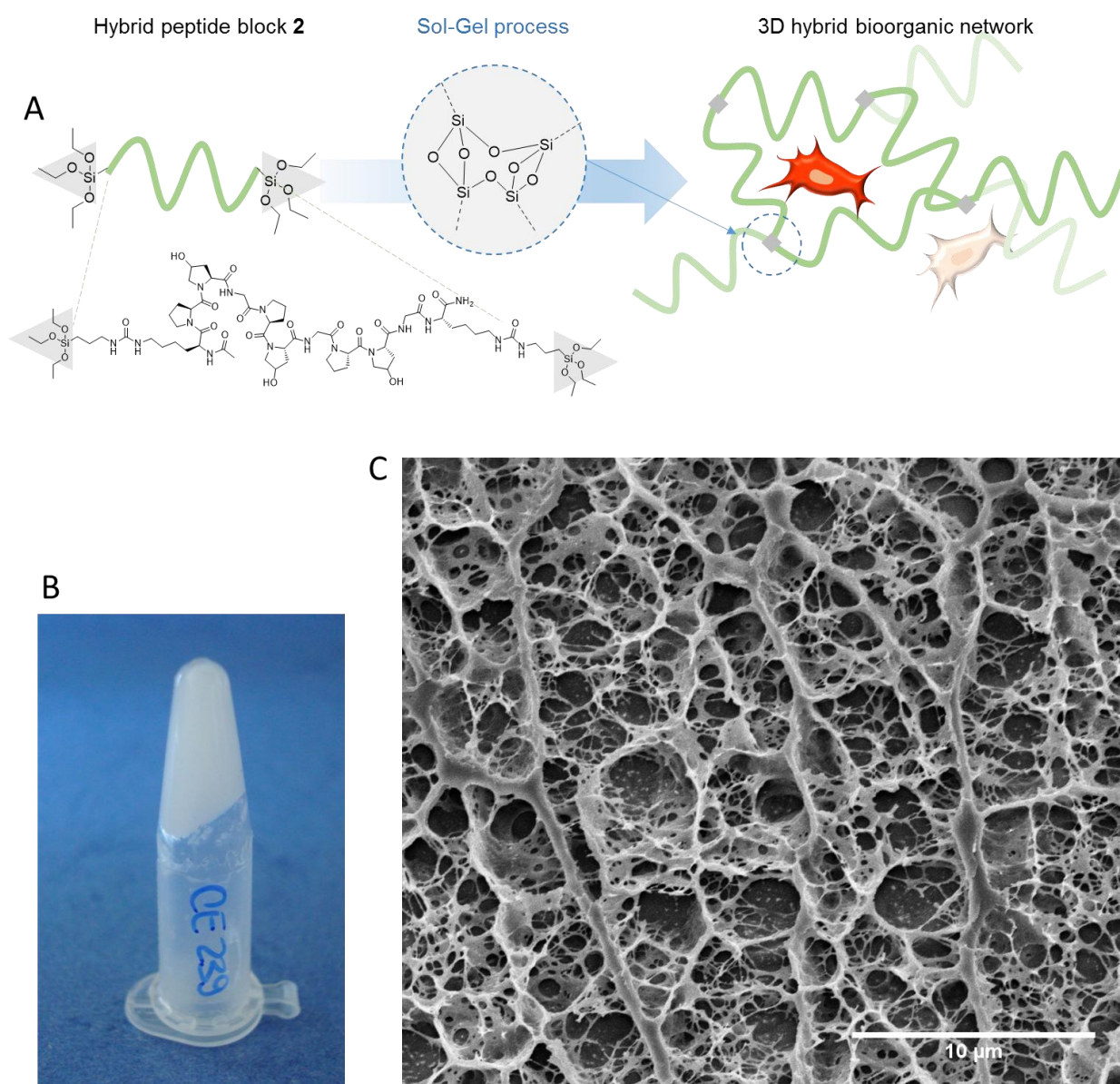


Figure 1. Schematic representation (A), photo (B) and cryo-SEM image (C) of the hybrid collagen-inspired hydrogel.

2. Materials and Methods

Silylation of peptide 1

Ac-Lys-[Pro-Hyp-Gly]₃-Lys-NH₂ was reacted with 3-isocyanatopropyltriethoxysilane (2.2 eq) in DMF at a concentration of 100 mM, in the presence of DIEA (4 eq) for 50 min. The bis-silylated hybrid block **2** was obtained after precipitation and washings with diethyl ether.

Collagen-inspired hybrid hydrogel preparation

The hybrid peptide **2** (200 mg) was dissolved in 10% FBS supplemented DMEM (Gibco, ref. 31966, 2 mL) at a 10 wt% concentration. The solution was filtered on a 0.22 μm pore size

filter. Sodium fluoride (0.3 wt%, 6 mg) was added. The hybrid solution was incubated at 37 °C overnight to yield the hybrid hydrogel.

Peptide synthesis protocols, NMR studies, rheology, SEM images, CD spectra and cell culture assays are fully detailed in supplementary information.

3. Results and discussion

3.1. Synthesis of a bis-silylated undecapeptide as hydrogel building block

A convergent synthesis was first set up to prepare the undecapeptide **1**. It involved the synthesis of the Fmoc-Pro-Hyp-Gly-OH tripeptide in solution, and its use as a building block for the stepwise synthesis on solid support (S.I. figure S1). In the meantime, we developed a novel methodology for rapid peptide synthesis called Fast Parallel Peptide Synthesis (FPPS).[29] This methodology was successfully applied to the synthesis of peptide **1** that was obtained in only 3 hours (Figure 2, S.I. p S3).

After N-terminus acetylation, the peptide **1** was cleaved from the resin concomitantly with the removal of the N-terbutyloxycarbonyl (Boc) and t-butyl ester (tBu) groups, which protected respectively the side chains of lysine and hydroxyproline residues. At this stage, compound **1** has been purified by RP-preparative HPLC (yield 50%, > 99% purity). The synthesis was repeated several times and the large-scale RP-HPLC purification was optimized (S.I. p S3). The overall process proved to be robust enough to provide multi-gram batches of pure peptide **1**. The key step of the synthesis was the introduction of the two alkoxy silane moieties. N-ε amino groups of lysine residues reacted quantitatively with 3-isocyanatopropyltriethoxysilane (ICPTES) in the presence of DIEA, to yield the bis-functionalized undecapeptide **2** (Figure 2). The hybrid peptide building block **2** was recovered quantitatively by precipitation in diethyl ether and characterized by ¹H, ¹³C, ²⁹Si NMR, and LC/MS (S.I. figures S3-S7).

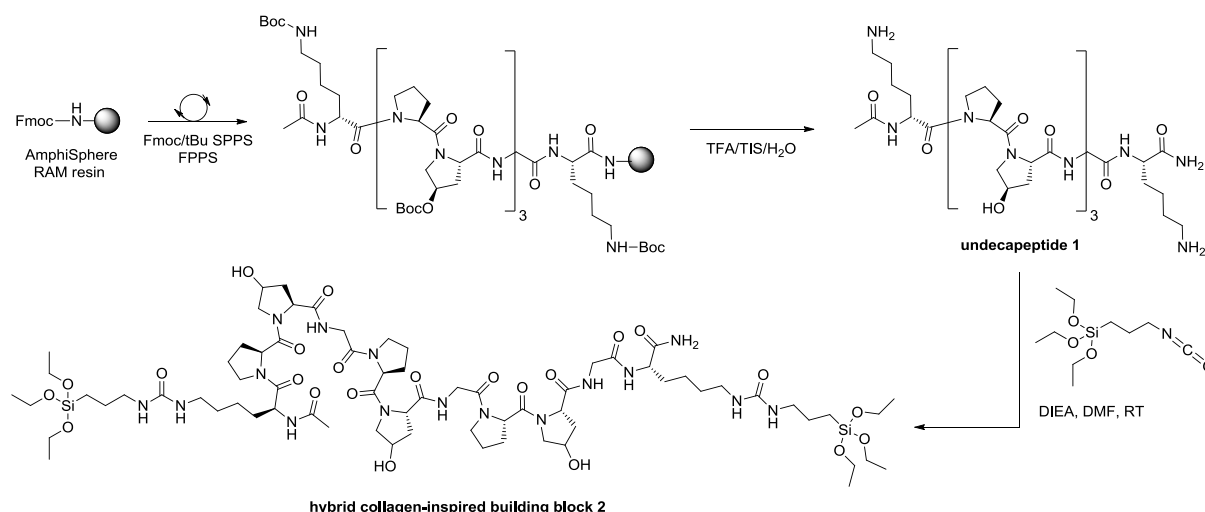


Figure 2. Synthesis of the hybrid bis-silylated undecapeptide **2**, Ac-Lys[CONH-(CH₂)₃-Si(OEt)₃]-[Pro-Hyp-Gly]₃-Lys[CONH-(CH₂)₃-Si(OEt)₃]-NH₂

We investigated the propensity of the short peptide sequence of **2** to adopt a PPII helix structure and self-assemble in triple helix by circular dichroism (CD) and NMR spectroscopies in DPBS buffer, pH 7.2. The CD spectrum of **2** showed a typical PPII signature with negative and positive maxima at 200 and 224 nm, respectively (S.I. Figure S13). Moreover, characteristic NOE correlations of the PPII helical fold were found on the ROESY spectrum of **2** (i.e, strong and medium $H\alpha(i),H\delta(i+1)$ and $H\beta(i),H\delta(i+1)$ NOE peaks). In this context, the three Pro-Hyp-Gly repeats adopt a PPII while the lysine residues and the silylated arms were disordered since few NOEs could be detected in these moieties, as expected. The building block has a maximal dimension of 66 Å, with a length of 26 Å for the PPII secondary structure. Finally, the 1H resonances of **2** were similar at 62 mM and 0.62 mM (10 and 0.1 wt%, respectively) showing that this undecapeptide was too short to assemble in triple helix (S.I. Figure S9).

3.2. Hydrogel formation

The sol-gel process consists in the hydrolysis of alkoxy-silyl groups followed by condensation to yield siloxane bonds.[30] Depending on the conditions (e.g. pH, catalyst) these two processes happen either sequentially or concomitantly. Cross-linked hydrogels of biopolymers such as gelatin,[31] alginate[32], chitosan,[33] and hydroxypropylmethyl cellulose (HMPC)[34] have already been obtained by the sol-gel process. However, such protocols involve either a pH solution that is not compatible with live cells or toxic chemical reagents that have to be removed prior to biological assays. Alternatively, they are based on hydrolysis of the alkoxy-silanes in acidic or basic conditions, followed by condensation upon neutralization of the medium. The method we have developed proceeds at 37°C, at physiological pH (7.4), in suitable biological buffer (DPBS or DMEM). It could be compatible with the inclusion of stem cells and, more importantly, could allow injection, and *in vivo* gelation.[35]

Accordingly to our previous study,[16] sodium fluoride was used to catalyse both the condensation, and the hydrolysis process (S.I. figure S8 A and B respectively), at physiological pH. Each of the silane group of the hybrid collagen peptide might undergo three successive condensations to yield three Si-O-Si bonds, which might link the same pair of atoms. Such 'intra' condensation can be considered as a linear enlargement of the polymeric chain. Alternatively, each silicon atom can be linked to two or three different partners. In this case, a reticulation node was created which can be considered as a chemical cross-link between the polymer chains. Hence, a covalent three-dimensional network was established, made of short (Pro-Hyp-Gly)₃ sequences linked by siloxane bonds (Figure 1).

In practice, building block **2** was dissolved in cell culture medium (62 mM in DMEM with 10% FBS), at a concentration of 10 wt%. 0.3 wt% of sodium fluoride was added and the hybrid solution was placed at 37°C to form a gel. The evolution of the sol-gel process was monitored by liquid 1H NMR. For this study, cell culture medium was replaced by DPBS (DPBS \times 10/D₂O/H₂O 1/1/8 v/v/v). The hybrid solution was introduced in a NMR tube and spectra were performed at 37°C (Figure 3 and S.I. pp S9-S13). The hydrolysis of ethoxysilanes was monitored by quantification of the released ethanol. Based on the integration of the CH₃ signal of EtOH, it appeared clearly that 70% of SiOEt groups were hydrolysed after 5 minutes. The hydrolysis was found to be complete after 60 min. These results were also confirmed by the disappearance of the signal attributed to -Si(OCH₂CH₃)₃. Since the hydrolysis and the polycondensation reactions operated at the same time under nucleophile (F⁻ herein) catalyst, a regular decrease of the overall signal of peptide was also observed, resulting from the disappearance of free peptides in solution upon condensation. No precipitation was observed but the solution turned into a gel after 90 minutes. It is worth

noting that the condensation was incomplete even after several hours, due to the gelation which limited the movement of polymer chains.

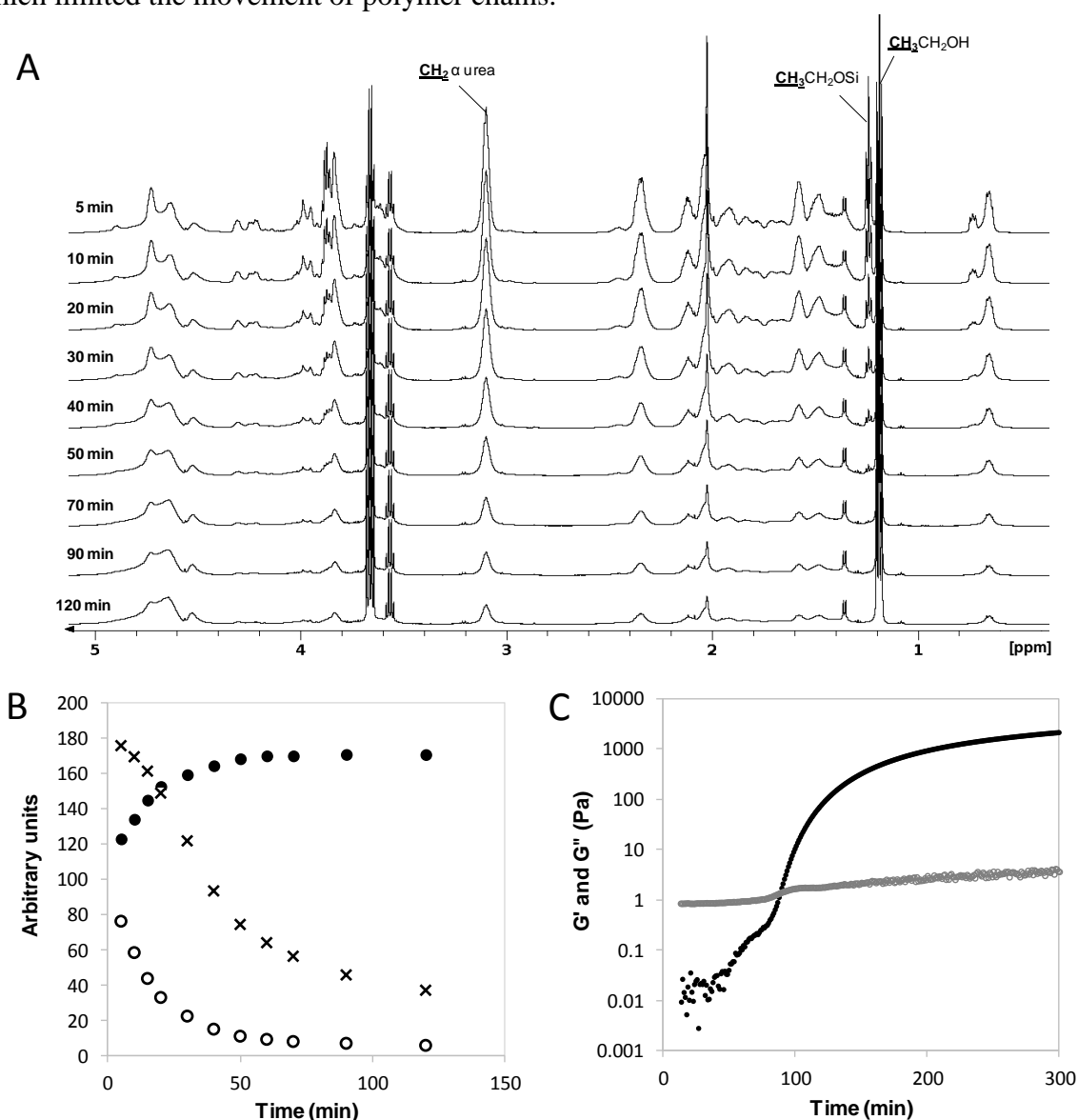


Figure 3. Monitoring of hydrogel formation by ^1H NMR and rheology. A: ^1H NMR spectra of the hybrid peptide **2** at a 10 wt% concentration in DPBS containing 0.3 wt% of NaF. B: Integration of ^1H NMR signals of the CH_3 group of ethanol ($\delta = 1.18$ ppm, ●), $\text{Si}(\text{OCH}_2\text{CH}_3)_3$ of the hybrid peptide ($\delta = 1.24$ ppm, o) and CH_2 groups of the hybrid peptide located in α position of ureas ($\delta = 3.10$ ppm, x). C: G' (●) and G'' (o) moduli measured on a hybrid peptide **2** solution (10 wt% in cell culture media containing 0.3 wt% of NaF) at 37°C (25% strain, 1 Hz).

The gelation process was also monitored by rheology in order to determine the gel point (Figure 3, C). The viscoelastic behavior of a system is characterized by the storage (G') and loss (G'') moduli which respectively quantify the solid-like and fluid-like contributions to the measured response when a sinusoidal shear deformation is applied to the system. Oscillatory shear measurements were performed on the hybrid peptide **2** solution (10 wt% in cell culture media with 0.3 wt% of NaF) at 37°C using an AR 2000 rheometer (TA Instruments, Inc) with a 20 mm diameter parallel geometry. The hybrid solution was deposited on the Peltier plate

and the gap was set at 500 μm . The dependence of G' and G'' moduli was measured as a function of time within the linear viscoelastic regime of the hydrogel (25% strain, 1 Hz). Initially, G'' was greater than G' which indicated a viscous behavior of the sample. During the experiment, G' increased quickly due to the formation of elastic intermolecular cross-links upon polycondensation while G'' increased negligibly. Thus a crossover of G' and G'' was observed at 90 min corresponding to the gel point. Afterwards, the sample presented solid-like properties. Frequency sweep experiment was also carried out and showed no dependence of the G' modulus as a function of the frequency at 25% strain. (S.I. figure S14).

These hybrid hydrogels were examined by Scanning Electron Microscopy (SEM). Images obtained in wet state by environmental SEM or after freeze-drying and gold coating by conventional SEM were not satisfactory due to either a low resolution or the denaturation of the hydrogel during the freeze-drying process (S.I. figure S15). We then turn our attention to cryoSEM technique which enables to freeze the inner structure of the hydrogel. Only a thin layer of water is removed from the sample to observe its surface. Interestingly, cryoSEM images showed a homogeneous porous matrix all over the different samples. Interestingly, micrometric alveoli were observed (Figure 1C and S.I. figure S16), whose size was comparable to alveoli obtained in elastin porous hydrogels.[36] The size of the pores suggested that collagen-inspired hydrogels could be suitable for the inclusion of cells.

3.3. Biological assessment

Cell adhesion and proliferation properties of hybrid (Pro-Hyp-Gly)₃-based hydrogels were assayed using mouse mesenchymal stem cells (mMSC). This cell line was chosen in the perspective of tissue engineering applications. Indeed, MSC are a promising alternative to chondrocytes to treat osteoarthritis or other osteochondral defects, a major cause of disability and pain among the ageing population.[37] MSC are the most attractive stem cells for cartilage repair,[38] as they can be readily isolated from various tissues such as bone marrow, adipose tissue, umbilical cord, synovia and synovial fluid. These cells are characterized by their capacity to differentiate into three main lineages, bone, fat, and cartilage. On the contrary to chondrocytes, they can be isolated and expanded quite easily. To optimize their differentiation, to improve their viability and to limit their dissemination after implantation, it is highly important to associate the MSC with a support.[39]

Cell adhesion

The hybrid collagen-inspired peptide **2** was dissolved in cell culture media at a concentration of 10 wt%, in the presence of sodium fluoride (0.3 wt%). The hybrid solutions were poured into 96-well cell culture plates, and incubated overnight at 37°C. The resulting hydrogels were washed with cell culture media, and mMSC were seeded onto their surface. Adherent cells were quantified with the CellTiter-Glo luminescent cell viability assay after 30 min, 1 h, 2 h, and 4 h (Figure 4, A). These results were compared to cell adhesion on tissue culture polystyrene (TC-PS), and commercially available foams made of cross-linked type I bovine collagen (ACE surgical). As expected, the number of cells measured out on bovine collagen foams after washing was very high, since cells could be retained in their porous structure. Interestingly, cell adhesion on hybrid peptide gels was more efficient than on TC-PS, and increased as a function of time. After 4 hours of contact between cells and substrates, cell attachment on hybrid peptide gels was more than twice higher than on TC-PS, and interestingly was equivalent to the cell attachment on commercially available collagen foams.

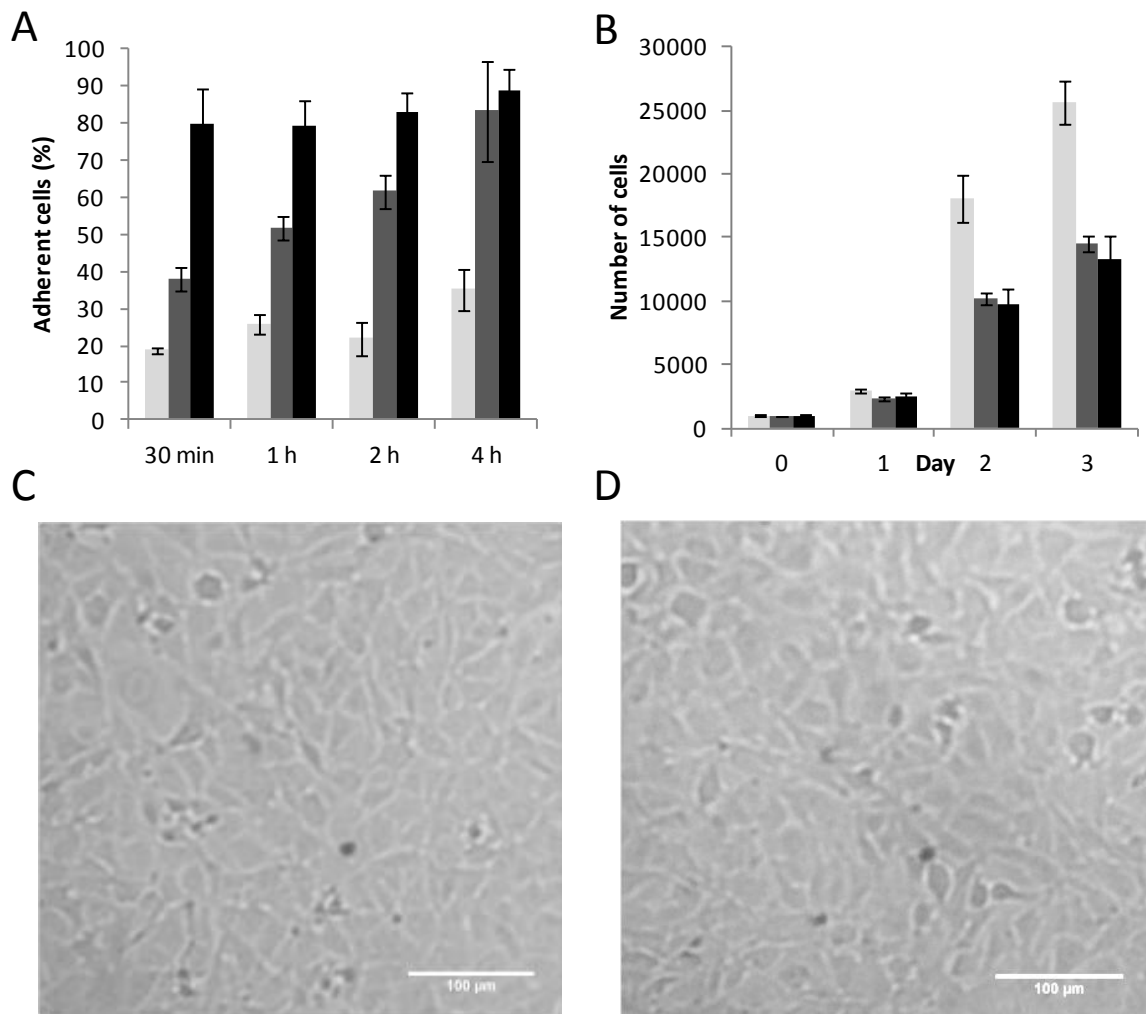


Figure 4. mMSC adhesion (A) and proliferation (B) on TC-PS (light grey), on hybrid collagen-inspired peptide **2** hydrogels (dark grey) and on commercially available bovine collagen foams (black). Microscopic images of cells after 3 days of culture on TC-PS (C) and on hybrid collagen-inspired peptide **2** hydrogel (D).

Cell proliferation

Encouraged by the cell attachment results, we investigated the cell proliferation on the surface of hybrid gels. Gels were prepared according to the procedure described above for adhesion assays. TC-PS and commercially available bovine collagen foam were used as controls. mMSC were seeded on the surface of the samples, and allowed to proliferate until confluence was reached on the TC-PS control. Every day, cells were quantified with the CellTiter-Glo assay (Figure 4, B). The cell proliferation on hybrid peptide hydrogels was as efficient as on bovine collagen foams. To complement the proliferation assay, direct optical microscopy observation was performed on TC-PS and hybrid gels which were transparent. Such direct observation was not possible on the collagen foams because of their opacity. Although the number of cells on hybrid gels was lower than on TC-PS by the end of the experiment, microscopic observations showed that cells had reached confluence in both cases (Figure 4, C and D). A possible explanation for this phenomenon was that the meniscus shape of the gel surface prevented cells from migrating to the edges of the gels, thus reducing the available surface for proliferation.

Cell encapsulation

After demonstrating that cells could proliferate at the surface of hybrid gels, we wanted to take advantage of the sol-gel process to encapsulate live cells in the hybrid gels before the gel point. mMSC were seeded in a hybrid peptide **2** solution with the same composition as previously (10 wt% of **2** in cell culture media with 0.3 wt% NaF). After 25 hours of incubation, cells were stained with a Live/Dead assay kit and their viability was checked by observation with a fluorescent microscope. Live cells appeared in green (calcein) while dead cells were stained in red (EthD-III). On the first attempt, most cells died. However, after decreasing the amount of sodium fluoride from 0.3 wt% to 0.01 wt%, the viability of the stem cells in the hybrid gels was fully conserved (Figure 5). Confocal microscopy images showed that cell distribution was rather homogeneous, except in the area impacted by the meniscus of the gel surface.

Noteworthy, special attention has to be paid to sodium fluoride concentration. Cell-free hydrogels are attractive as cell culture supports or as implantable materials aiming at filling a gap or a defect inside native tissues, which are further colonized by endogenous cells. Hydrogel dressings[40] or scaffold designed for spinal cord injuries[41] fall in this category. For such applications, hydrogels can be washed before putting them in contact with living cells and thus a high concentration in sodium fluoride, even cytotoxic, can be used to increase the gelation speed. However, when cells are embedded in the hydrogel matrix, a low NaF concentration should be preferred. These conditions decrease the gelation rate. As a consequence, in our study, the hybrid peptide solution was prepared 17 hours before cell seeding. At this point, the mMSC were suspended in the viscous solution and did not sediment during the 25 h-incubation, as witnessed by the lateral microscopic view (Figure 5, C). The good cell viability observed using this procedure enlarge the range of potential applications of hybrid peptide hydrogels to cell-laden matrixes.

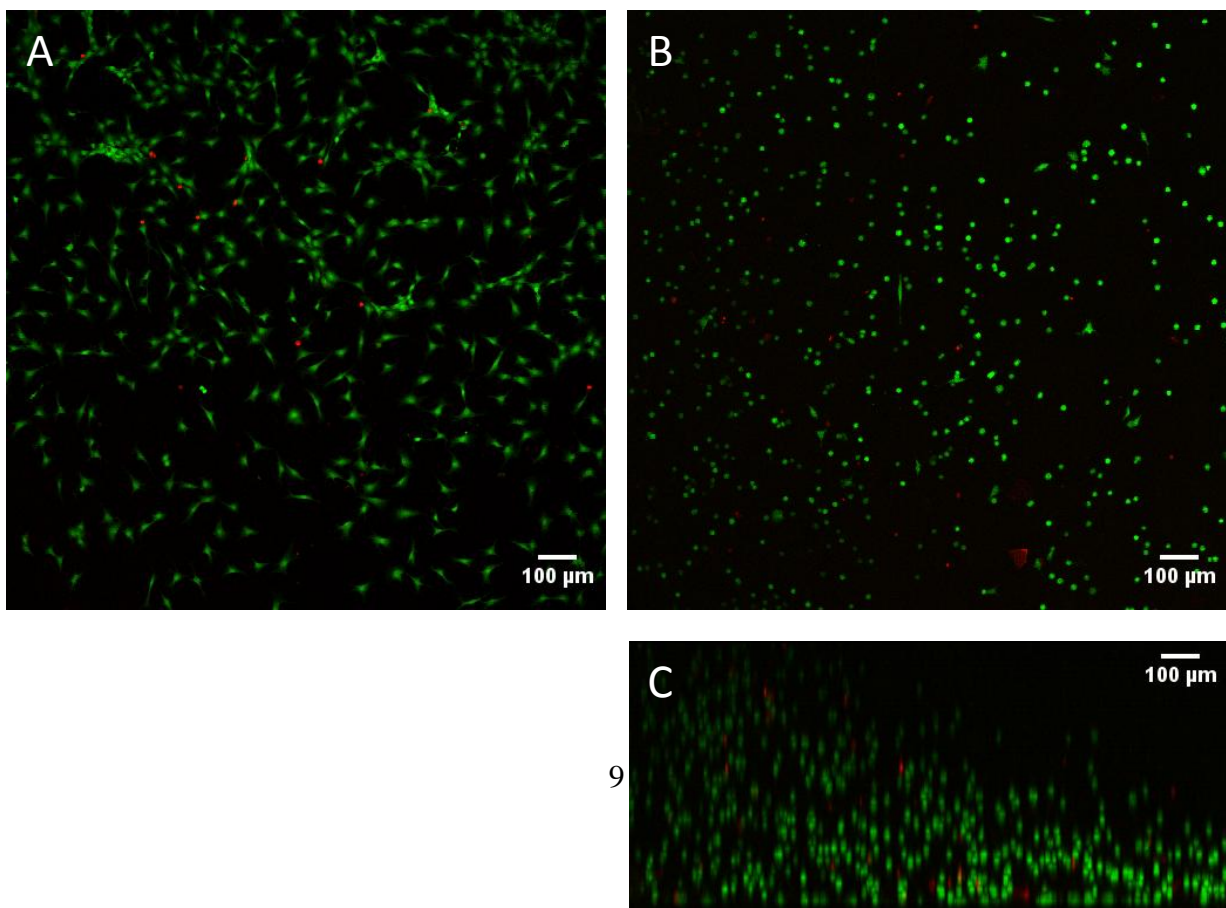


Figure 5. Confocal microscopy images of mMSC 25h after seeding. (A) top view of a 2D-culture on TC-PS. (B) top view (z-projection) and (C) side view (y-projection) of a 3D-culture inside a hybrid collagen-inspired peptide hydrogel.

4. Conclusion

In contrast to natural collagen scaffolds, the use of a short bis-silylated peptide to prepare biocompatible hydrogels presents several interesting features. Firstly, the technology offers the possibility to create biocompatible gels from a synthetic starting material, which is of a paramount interest in terms of safety, cost of production and putative translation to the clinics. Secondly, the NaF catalyzed sol-gel process we described is straightforward and proceeds entirely in biological media. The sol-gel process has already been exploited to form hydrogels from biopolymers such as chitosan,[33] gelatin[31] and modified-cellulose,[34] that were cross-linked by silylation with 3-(glycidoxypropyl)trimethoxysilane. However, in these studies, the hydrolysis was performed in strong acidic or basic media, and condensation occurred either at a pH non-compatible with cell survival, or separately from hydrolysis upon careful neutralisation. In addition, the fact that the mixture containing hydrogel precursors, nutrients, factors and cells can be handled as a solution, is of great advantage when injection is required, or even when scaffold 3D printing is envisioned. Biofabrication using different silylated bioinks that could polymerize simply by the sol-gel process is of great significance for future developments. It is important to notice that the nature of the silanol chemistry itself unlocks the possibility to design and synthesize multifunctional and tailored hydrogels. In fact, Si-O-Si bond formation is chemoselective, but it is also a ‘symmetrical’ reaction, involving the same reactive moiety, several times. This represents a ground breaking improvement over systems of chemical cross-linking such as maleimide/thiol[11] or photoactivation,[42] which involve two different chemical groups. Although the Si-O-Si bond formation does not allow the control of directed assemblies (e.g. regular formation of -A-B-A-B- from A and B blocks), a single type of functionalization is sufficient to get a covalent network bringing together any type of silylated building blocks (i.e. polymers, peptides, fluorophores, drugs, etc.). The control of the cross-linking degree could be easily tuned by varying the length of precursors but also by introducing tri or tetra-silylated molecules. Taking into account the diversity of natural tissues in terms of biochemical composition and structural features, a versatile and generic method to build dedicated hydrogels is of high interest. In this perspective, the hybrid collagen-inspired peptide forming hydrogel is a promising brick for the straightforward synthesis of biomimetic structures.

Acknowledgements

C. Echalié's PhD was partly funded by the “Region Languedoc Roussillon”, grant attributed to G. Subra, through the program ‘Chercheur d’Avenir’. Peptide syntheses were performed using the facilities of SynBio3 IBISA platform supported by IBMM and ITMO cancer. Cryo-SEM analyses were realized by the CT μ (Centre technique des microstructures) from EZUS-Lyon 1 University. Karine Toupet and Gautier Tejedor performed confocal microscopy

observations, using the facilities of the Institute for Regenerative Medicine and Biotherapy (IRBM, Montpellier).

References

- [1] M. Taba, Q. Jin, J.V. Sugai, W.V. Giannobile, *Orthod. Craniofac. Res.* 8 (2005) 292–302.
- [2] R.A. Barry, R.F. Shepherd, J.N. Hanson, R.G. Nuzzo, P. Wiltzius, J.A. Lewis, *Adv. Mater.* 21 (2009) 2407–2410.
- [3] A. Cretu, P. Castagnino, R. Assoian, *J. Vis. Exp. JoVE* (2010).
- [4] M. Guvendiren, J.A. Burdick, *Biomaterials* 31 (2010) 6511–6518.
- [5] C.-C. Lin, *RSC Adv.* 5 (2015) 39844–39853.
- [6] U. Hersel, C. Dahmen, H. Kessler, *Biomaterials* 24 (2003) 4385–4415.
- [7] C.-Y. Lin, Y.-R. Wang, C.-W. Lin, S.-W. Wang, H.-W. Chien, N.-C. Cheng, W.-B. Tsai, J. Yu, *BioResearch Open Access* 3 (2014) 297–310.
- [8] M. Patenaude, T. Hoare, *Biomacromolecules* 13 (2012) 369–378.
- [9] U. Freudenberg, J.-U. Sommer, K.R. Levental, P.B. Welzel, A. Zieris, K. Chwalek, K. Schneider, S. Prokoph, M. Prewitz, R. Dockhorn, C. Werner, *Adv. Funct. Mater.* 22 (2012) 1391–1398.
- [10] M.V. Tsurkan, K. Chwalek, S. Prokoph, A. Zieris, K.R. Levental, U. Freudenberg, C. Werner, *Adv. Mater.* 25 (2013) 2606–2610.
- [11] A. Watarai, L. Schirmer, S. Thönes, U. Freudenberg, C. Werner, J.C. Simon, U. Anderegg, *Acta Biomater.* 25 (2015) 65–75.
- [12] J.L. Vanderhooft, M. Alcoutlabi, J.J. Magda, G.D. Prestwich, *Macromol. Biosci.* 9 (2009) 20–28.
- [13] J.W. Nichol, S.T. Koshy, H. Bae, C.M. Hwang, S. Yamanlar, A. Khademhosseini, *Biomaterials* 31 (2010) 5536–5544.
- [14] X. Hu, C. Gao, *J. Appl. Polym. Sci.* 110 (2008) 1059–1067.
- [15] Y.D. Park, N. Tirelli, J.A. Hubbell, *Biomaterials* 24 (2003) 893–900.
- [16] C. Echaliier, C. Pinese, X. Garric, H. Van Den Berghe, E. Jumas Bilak, J. Martinez, A. Mehdi, G. Subra, *Chem. Mater.* 28 (2016) 1261–1265.
- [17] S. Chattopadhyay, R.T. Raines, *Biopolymers* 101 (2014) 821–833.
- [18] L.B. Ensanya A Abou Neel, *Adv. Drug Deliv. Rev.* (2012).
- [19] Y. Feng, G. Melacini, J.P. Taulane, M. Goodman, *J. Am. Chem. Soc.* 118 (1996) 10351–10358.
- [20] F.W. Kotch, R.T. Raines, *Proc. Natl. Acad. Sci. U. S. A.* 103 (2006) 3028–3033.
- [21] M.A. Cejas, W.A. Kinney, C. Chen, G.C. Leo, B.A. Tounge, J.G. Vinter, P.P. Joshi, B.E. Maryanoff, *J. Am. Chem. Soc.* 129 (2007) 2202–2203.
- [22] M.A. Cejas, W.A. Kinney, C. Chen, J.G. Vinter, H.R. Almond, K.M. Balss, C.A. Maryanoff, U. Schmidt, M. Breslav, A. Mahan, E. Lacy, B.E. Maryanoff, *Proc. Natl. Acad. Sci.* 105 (2008) 8513–8518.
- [23] C.L. Jenkins, R.T. Raines, *Nat. Prod. Rep.* 19 (2002) 49–59.
- [24] B. Saccá, L. Moroder, *J. Pept. Sci.* 8 (2002) 192–204.
- [25] J. Ottl, L. Moroder, *J. Am. Chem. Soc.* 121 (1999) 653–661.
- [26] V.A. Kumar, N.L. Taylor, A.A. Jalan, L.K. Hwang, B.K. Wang, J.D. Hartgerink, *Biomacromolecules* 15 (2014) 1484–1490.
- [27] L.E.R. O’Leary, J.A. Fallas, E.L. Bakota, M.K. Kang, J.D. Hartgerink, *Nat. Chem.* 3 (2011) 821–828.
- [28] J. Luo, Y.W. Tong, *ACS Nano* 5 (2011) 7739–7747.
- [29] G. Laconde, M. Simon, A. Messerschmitt, L. Vezenkov, J.-A. Fehrentz, G. Subra, J. Martinez, M. Amblard, Submitted (n.d.).

- [30] J. Zha, H. Roggendorf, *Adv. Mater.* 3 (1991) 522–522.
- [31] L. Ren, K. Tsuru, S. Hayakawa, A. Osaka, *J. Sol-Gel Sci. Technol.* 21 (2001) 115–121.
- [32] K. Hosoya, C. Ohtsuki, T. Kawai, M. Kamitakahara, S. Ogata, T. Miyazaki, M. Tanihara, *J. Biomed. Mater. Res. A* 71A (2004) 596–601.
- [33] Y. Shirosaki, C.M. Botelho, M.A. Lopes, J.D. Santos, *J. Nanosci. Nanotechnol.* 9 (2009) 3714–3719.
- [34] C. Vinatier, D. Magne, P. Weiss, C. Trojani, N. Rochet, G.F. Carle, C. Vignes-Colombeix, C. Chadjichristos, P. Galera, G. Daculsi, J. Guicheux, *Biomaterials* 26 (2005) 6643–6651.
- [35] M.K. Nguyen, D.S. Lee, *Macromol. Biosci.* 10 (2010) 563–579.
- [36] N. Annabi, S.M. Mithieux, A.S. Weiss, F. Dehghani, *Biomaterials* 30 (2009) 1–7.
- [37] E.A. Makris, A.H. Gomoll, K.N. Malizos, J.C. Hu, K.A. Athanasiou, *Nat. Rev. Rheumatol.* 11 (2015) 21–34.
- [38] C. Vinatier, D. Mrugala, C. Jorgensen, J. Guicheux, D. Noël, *Trends Biotechnol.* 27 (2009) 307–314.
- [39] M. Morille, K. Toupet, C.N. Montero-Menei, C. Jorgensen, D. Noël, *Biomaterials* 88 (2016) 60–69.
- [40] K. Murakami, H. Aoki, S. Nakamura, S. Nakamura, M. Takikawa, M. Hanzawa, S. Kishimoto, H. Hattori, Y. Tanaka, T. Kiyosawa, Y. Sato, M. Ishihara, *Biomaterials* 31 (2010) 83–90.
- [41] D. Tukmachev, S. Forostyak, Z. Koci, K. Zavisikova, I. Vackova, K. Vyborny, I. Sandvig, A. Sandvig, C.J. Medberry, S.F. Badylak, E. Sykova, S. Kubinova, *Tissue Eng. Part A* 22 (2016) 306–317.
- [42] J.W. Nichol, S.T. Koshy, H. Bae, C.M. Hwang, S. Yamanlar, A. Khademhosseini, *Biomaterials* 31 (2010) 5536–5544.

Supplementary Material

Sol-gel synthesis of collagen-inspired peptide hydrogel

Cécile Echalié, Said Jebors, Guillaume Laconde, Luc Brunel, Pascal Verdié, Léa Causse, Audrey Bethry, Baptiste Legrand, Hélène Van Den Berghe, Xavier Garric, Danièle Noël, Jean Martinez, Ahmad Mehdi and Gilles Subra**

Abbreviations	2
Material and Methods	2
Synthesis of undecapeptide 1	3
Silylation of undecapeptide 1	5
Preparation of a hydrogel	9
NMR study of 2 and monitoring of the gelation process	9
CD study	13
Rheology	14
Scanning Electron Microscopy	15
Cell adhesion	16
Cell proliferation	16
Encapsulation	17
Figure S1. Synthesis of undecapeptide 1 using Fmoc-ProHypGly-OH building block	3
Figure S2. LC/MS spectrum of 1	4
Figure S3. ¹H NMR spectrum of 2 in DMSO-<i>d</i>₆ (500 MHz)	5
Figure S4. ¹³C NMR spectrum of 2 in DMSO-<i>d</i>₆ (125 MHz)	6
Figure S5. ²⁹Si NMR spectrum of 2 in DMSO-<i>d</i>₆ (99 MHz)	6
Figure S6. LC/MS spectrum of 2	7
Figure S7. HR-MS analysis of 2	8
Figure S8. Proposed mechanism for fluorine-catalyzed sol-gel process. A: hydrolysis step. B: condensation step.	9
Figure S9. 1D ¹H NMR spectra of the hybrid peptide 2 at 62 mM and 0.62 mM (10 and 0.1%) in DPBS buffer (10% D₂O) without NaF at 37°C, pH 7.2.	10
Figure S10. 1D ¹H NMR spectra of the hybrid peptide 2 at 62 mM (10%) in DPBS buffer (10% D₂O) with and without NaF at 37°C, pH 7.2. Spectra were recorded after 5 and 60 min.	11
Figure S11. Nomenclature and chemical shifts for the silylated arm (R = -H or -CH₂CH₃)	12
Figure S12. 1D ¹H NMR spectra at different intervals of the hybrid peptide 2 at 62 mM (10%) in DPBS buffer (10% D₂O) with NaF at 37°C, pH 7.2.	13
Figure S13. CD spectrum of the hybrid peptide 2 (0.062 mM) in DPBS buffer, pH 7.2 at 37°C.	14
Figure S14. Frequency sweep from 10 to 0.1 Hz at 25% strain. Black dots: G'; Grey dots: G''	14
Figure S15. SEM image of a hydrogel (10 wt% of hybrid peptide 2 in DPBS with 0.3 wt% NaF) after freeze-drying	15
Figure S16. Cryo-SEM images of the hydrogel. A: before sublimation. B: after sublimation for 1 min at -96°C. C and D: after sublimation for 3 min at -87°C.	16

Abbreviations

ACN, acetonitrile; Boc, t-butyloxycarbonyl; BBOF, broad band fluorine observation; CD, circular dichroism; DIEA, diisopropylethylamine; DMEM, Dulbecco's modified eagle medium; DMF, N,N'-dimethylformamide; DMSO, dimethylsulfoxide; DPBS, Dulbecco's phosphate buffered saline; ECM, extracellular matrix; ESI-MS, electrospray ionization mass spectrometry; FBS, fetal bovine serum; Fmoc, fluorenylmethoxycarbonyl; FPPS, fast parallel peptide synthesis; HATU, *N*-[Bis(dimethylamino)methylene]-1H-1,2,3-triazolo[4,5-b]pyridinium 3-oxid hexafluorophosphate; HPMC, hydroxypropylmethylcellulose; ICPTES, 3-isocyanatopropyltriethoxysilane; LC/MS, tandem liquid chromatography/ mass spectrometry; mMSC, mouse mesenchymal stem cell; NIPAM, poly(*N*-isopropylacrylamide); NMR, nuclear magnetic resonance; pip, piperidine; PEG, polyethylene glycol; PHEMA, polyhydroxyethylmethacrylate; PLA, poly(lactic acid); PLGA, poly(lactic-co-glycolic acid); RP-HPLC, reversed phase high performance liquid chromatography; RT, room temperature; SEM, scanning electron microscopy; SPPS, solid phase peptide synthesis; TC-PS, tissue culture polystyrene; TFA, trifluoroacetic acid; TIS, triisopropylsilane; TMSP, trimethylsilyl-3-propionic acid 2,2,3,3-sodium salt; UV, ultra-violet, VEGF, vascular endothelial growth factor. Other abbreviations used were those recommended by the IUPAC-IUB Commission (Eur. J. Biochem. 1984, 138, 9-37).

Material and Methods

All solvents and reagents were used as supplied. Solvents used for LC/MS were of HPLC grade. DMF, DIEA, ACN, TIS, TFA and piperidine were obtained from Sigma-Aldrich. Fmoc amino acid derivatives and HATU were purchased from Iris Biotech (Marktredwitz, Germany). AmphiSpheres 40 RAM 0.37 mmol/g 75-150 μ m resin was purchased from Agilent Technologies. ICPTES and sodium fluoride were obtained from Alfa Aesar and Acros respectively.

Samples for LC/MS analyses were prepared in acetonitrile/water (50:50, v/v) mixture, containing 0.1% TFA. The LC/MS system consisted of a Waters Alliance 2695 HPLC, coupled to a Water Micromass ZQ spectrometer (electrospray ionization mode, ESI+). All the analyses were carried out using a Chromolith Flash 25 x 4.6 mm C18 reversed-phase column. A flow rate of 3 mL/min and a gradient of (0-100)% B over 2.5 min were used. Eluent A: water/0.1% HCO₂H; eluent B: acetonitrile/0.1% HCO₂H. UV detection was performed at 214 nm. Electrospray mass spectra were acquired at a solvent flow rate of 200 μ L/min. Nitrogen was used for both the nebulizing and drying gas. The data were obtained in a scan mode ranging from 100 to 1000 m/z or 250 to 1500 m/z to in 0.7 sec intervals.

High Resolution Mass Spectrometric analyses were performed with a Synapt G2-S (Waters) mass spectrometer fitted with an Electrospray Ionisation source. All measurements were performed in the positive ion mode. Capillary voltage: 1000 V; cone voltage: 30 V; source temperature: 120°C; desolvation temperature: 250°C. The data were obtained in a scan mode ranging from 0 to 2000 m/z.

NMR solvents and TMSP were obtained from Euriso-top. ²⁹Si, ¹³C and ¹H NMR spectra in DMSO-*d*₆ were collected on a Bruker AVANCE 500 MHz spectrometer equipped with a BBFO helium cryoprobe at 298 K. The deuterated solvent was used as an internal deuterium lock. Chemical shifts (δ) are reported in parts per million using residual non-deuterated solvents as internal references. Spectra were processed and visualized with Topspin 3.2 (Bruker Biospin).

Synthesis of undecapeptide 1

Convergent synthesis

A convergent synthesis strategy was first used to produce several grams of undecapeptide **1**. This strategy involved the solution phase synthesis of the Fmoc-ProHypGly-OH tripeptide. Boc-Hyp-OH was coupled on H-Gly-OBzl. Fmoc-Pro-OH was coupled on the resulting dipeptide after Boc removal in TFA. Removal of C-ter protecting group by catalyzed hydrogenation yielded the tripeptide ready to use as a building block for the synthesis of the undecapeptide **1**.

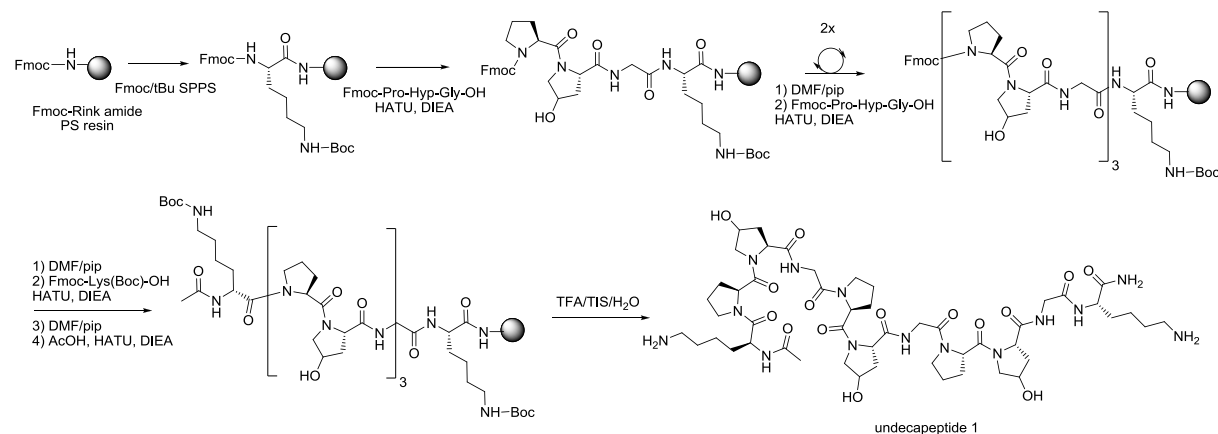


Figure S1. Synthesis of undecapeptide **1** using Fmoc-ProHypGly-OH building block

After purification, the undecapeptide **1** was obtained with 45% yield.

FPPS synthesis

The FPPS methodology developed in our group (Laconde, G. *et al.* Fast parallel peptide synthesis - FPPS: A methodology for the rapid and efficient preparation of peptide libraries. *Submitted*) was also applied to the synthesis of undecapeptide **1**. All the stages of the FPPS were realized under vortex stirring at 500 rpm, on a 0.5 mmol scale using the AmphiSpheres 40 RAM (0.37mmol/g 75-150) μ m resin in DMF. Stock solutions of all Fmoc-protected amino acids (Fmoc-Lys(Boc)-OH, Fmoc-Gly-OH, Fmoc-Hyp(tBu)-OH, Fmoc-Pro-OH) and HATU were prepared in DMF at 0.5 M. The coupling reactions were performed using a amino acid (5 ml, 5 eq) / HATU (5 ml, 5 eq) / DIEA (0.87 ml, 10 eq) mixture for 5 minutes and repeated twice. Fast double couplings were replaced by a single 30 min coupling for Fmoc-Hyp(tBu)-OH. The Fmoc removal steps were realized using a piperidine/DMF 20/80 v/v solution (12 ml) for 1 minute and performed twice. All washings were done with DMF (12 ml). N-Terminal acetylation was performed with 20% Ac₂O in DMF and DIEA for 5 minutes twice. The peptide was cleaved from the resin with the cocktail TFA/TIS/H₂O (95/2.5/2.5 v/v/v), recovered by precipitation in diethyl ether, then taken up in ACN/H₂O 50/50 v/v mixture and freeze-dried.

The crude peptide was solubilized in H₂O/ACN 98/2 v/v mixture with 1% TFA and purified by RP-preparative HPLC. The purification was performed on a NOVASEP HPLC system equipped with a C18 reversed-phase Luna column (Phenomenex 10 μ m, 250 \times 50 mm) with a flow rate of 120 mL/min. Eluents were H₂O 1% TFA (A) and ACN 1% TFA (B). The purification gradient started with 3 minutes at 0% of B and then increased from 0 to 20% of B in 20 min. UV detection was performed at 221 nm. Collected fractions were concentrated and freeze-dried to yield the pure undecapeptide **1** as a TFA salt with 50% yield. This yield was similar to the yield of the convergent strategy. However, the synthesis of the peptide was much faster with the FPPS methodology. As a consequence, this protocol was selected for large-scale synthesis of peptide **1**.

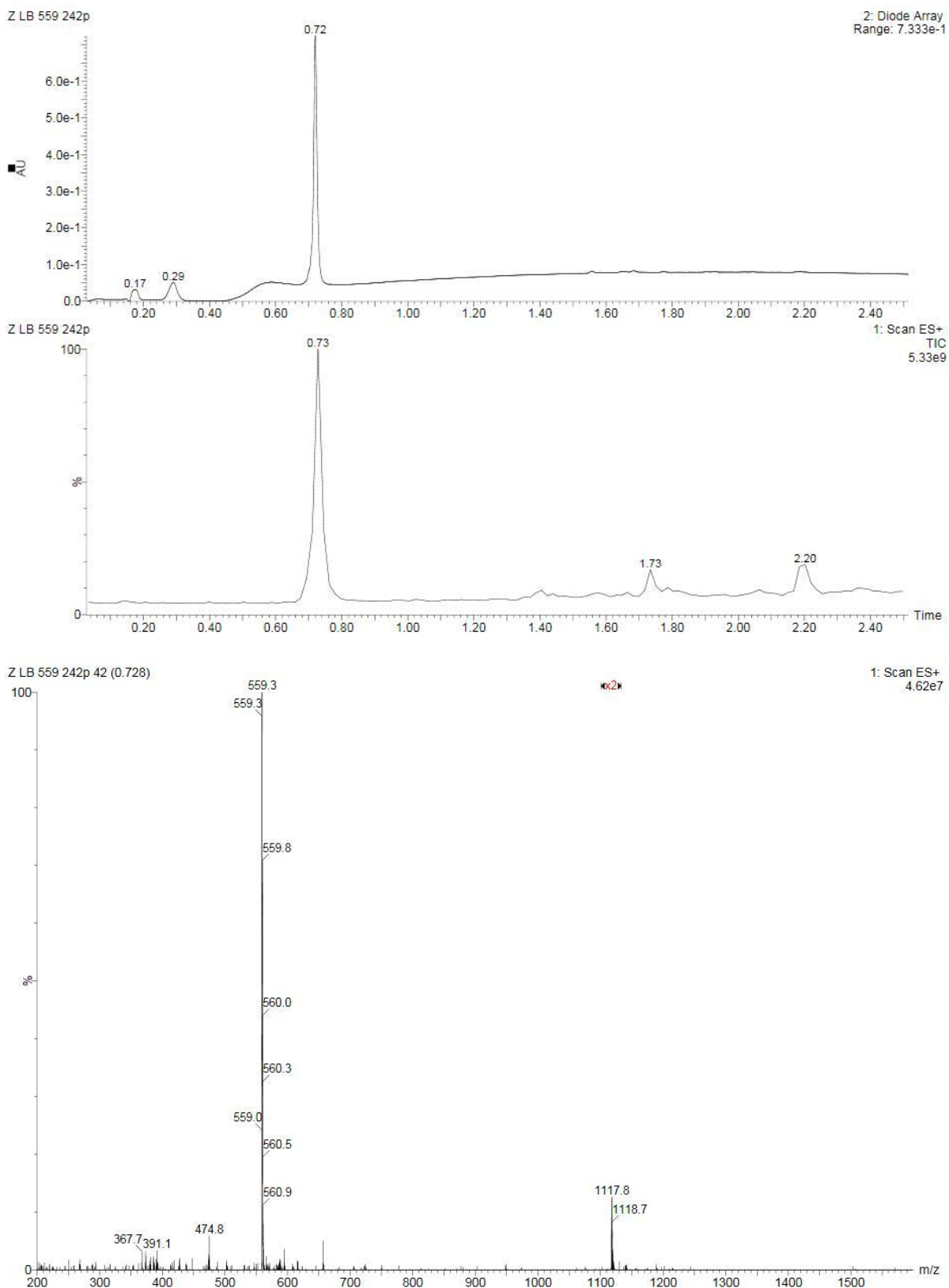


Figure S2. LC/MS spectrum of **1**

LC/MS (ESI⁺): t_R = 0.72 min, m/z 1118 ([M+H]⁺, 8%), 559 ([M+2H]²⁺, 100)

Silylation of undecapeptide **1**

Undecapeptide **1** was reacted with 3-isocyanatopropyltriethoxysilane (2.2 eq) in anhydrous DMF at a concentration of 100 mM in the presence of DIEA (4 eq) for 50 min under argon atmosphere. The completion of the reaction was checked by HPLC. The bis-silylated hybrid block **2** was obtained quantitatively after precipitation and washings with diethylether.

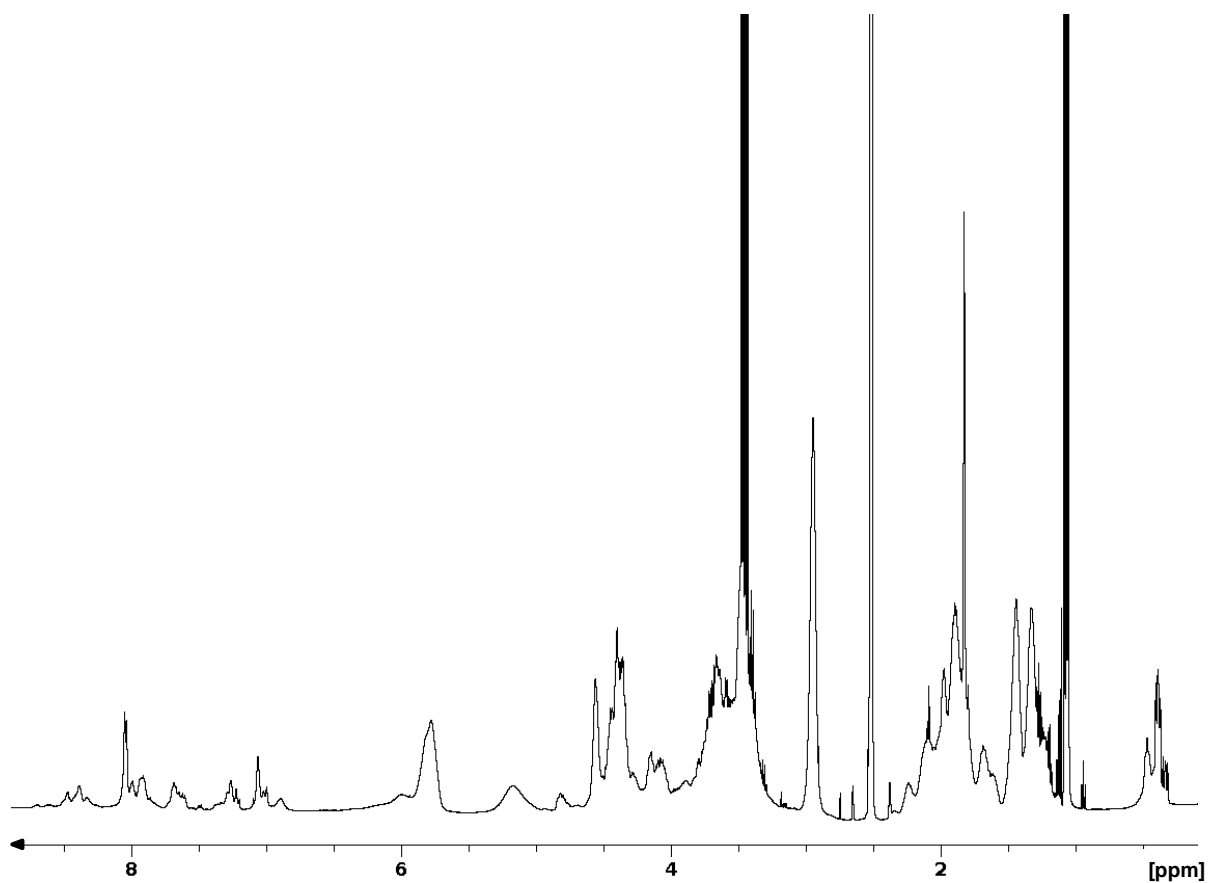


Figure S3. ¹H NMR spectrum of **2** in DMSO-*d*₆ (500 MHz)

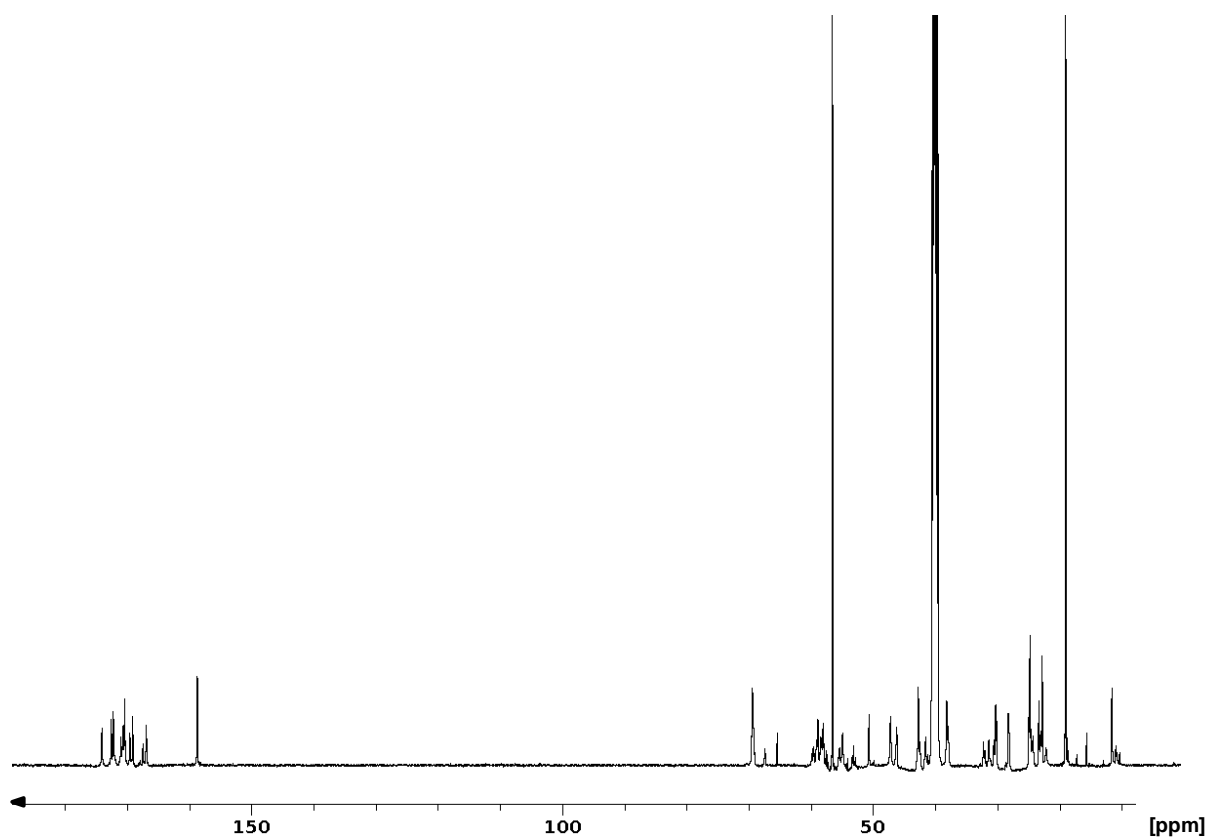


Figure S4. ^{13}C NMR spectrum of **2** in $\text{DMSO-}d_6$ (125 MHz)

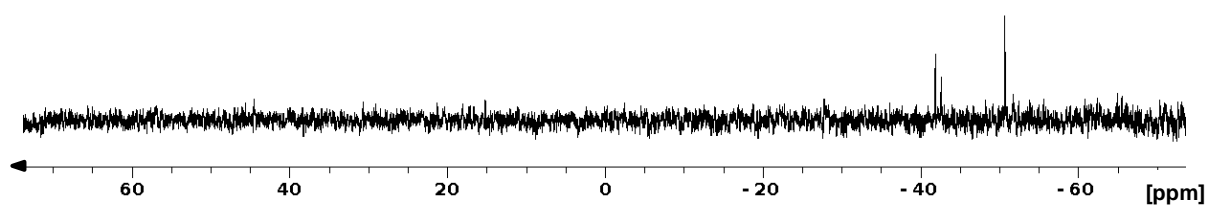


Figure S5. ^{29}Si NMR spectrum of **2** in $\text{DMSO-}d_6$ (99 MHz)

Noteworthy, 3 signals are observed on the ^{29}Si NMR spectrum corresponding to different states of hydrolysis and condensation of $-\text{Si}(\text{OEt})_3$ groups.

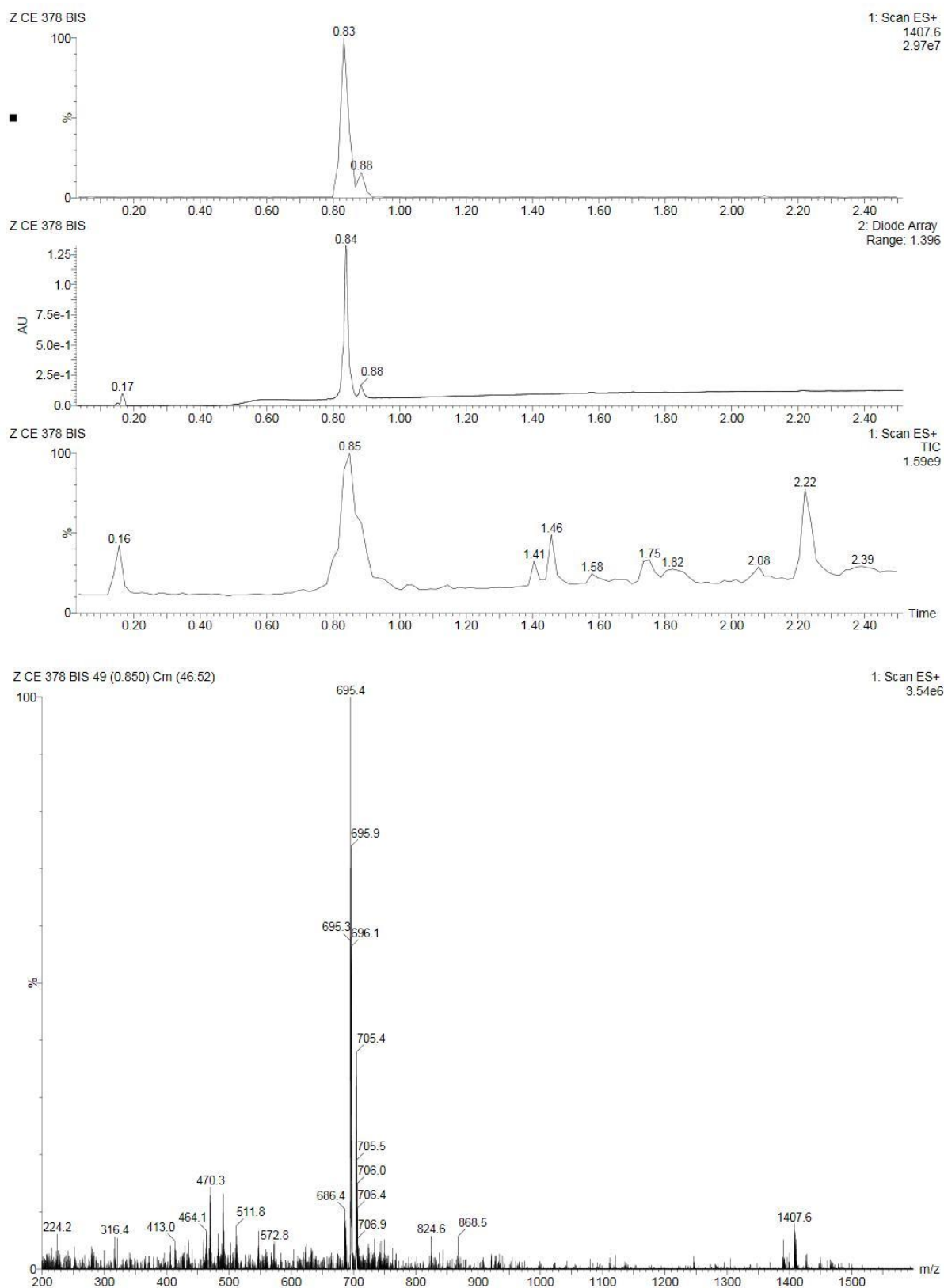


Figure S6. LC/MS spectrum of **2**

LC/MS (ESI⁺): Only the product of hydrolysis of ethoxysilyl groups into silanols is detected with several H₂O losses. *t*_R = 0.84 min, *m/z* 1408 ([M-2H₂O+H]⁺, 10%), 695 ([M-3H₂O+2H]²⁺, 100).

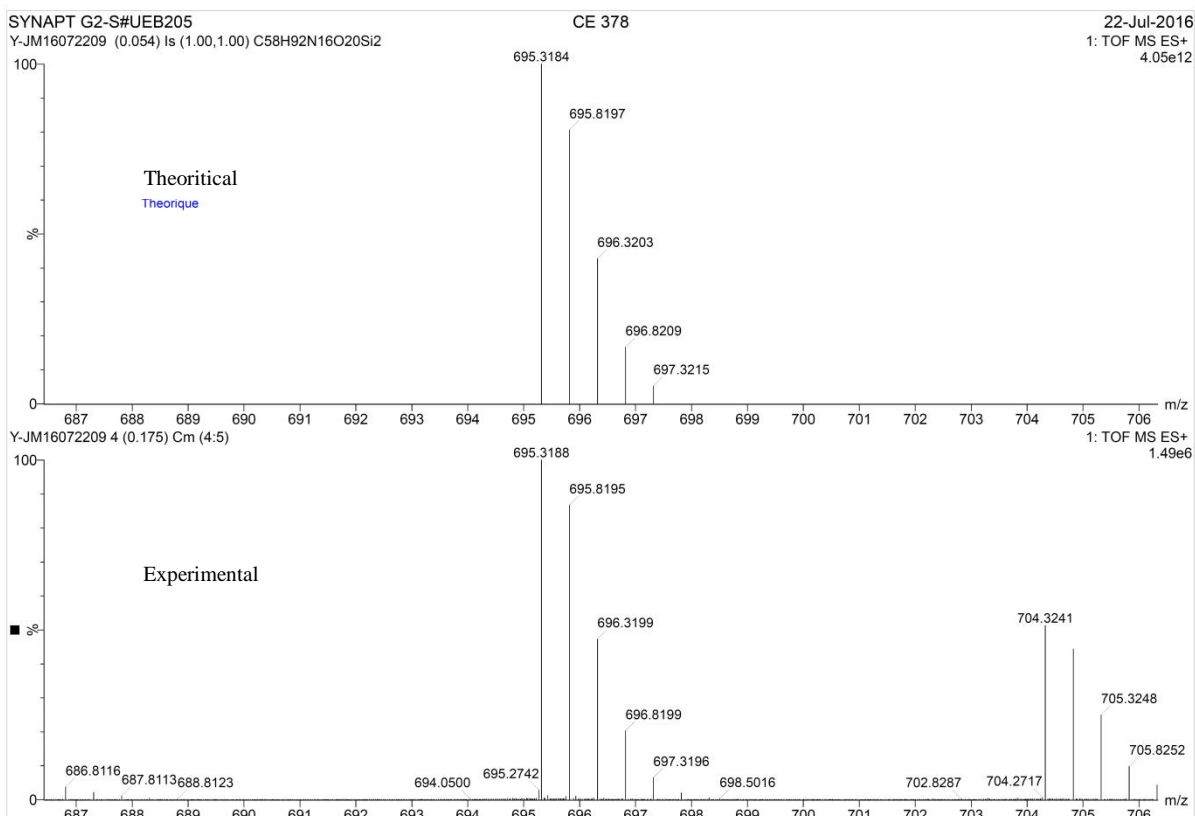
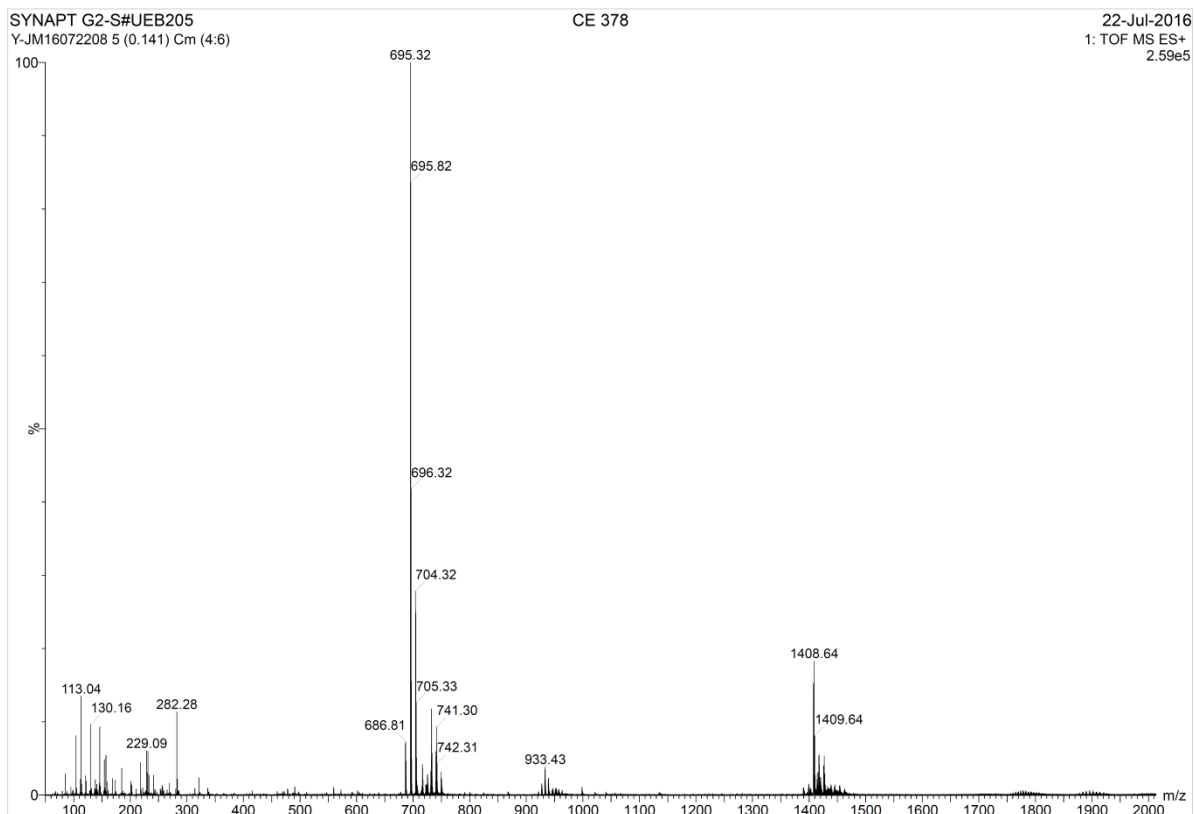


Figure S7. HR-MS analysis of **2**

HR/MS (ESI⁺): Only the product of hydrolysis of ethoxysilyl groups into silanols is detected with several H₂O losses. It is usual to observe $-\text{Si}^+(\text{OH})_2$ species when hybrid derivatives are analyzed by

ESI⁺ MS. The most abundant ion at $m/z = 695.3188$ corresponds to $[M-3H_2O+2H]^{2+}$ with M the hydrolyzed hybrid peptide.

Preparation of a hydrogel

Hybrid bloc **2** (200 mg) was dissolved in 10% FBS supplemented DMEM (Gibco, ref. 31966, 2 mL) at a 10 wt% concentration. The solution was filtered on a 0.22 μm pore size filter to sterilize the solution when required. Sodium fluoride (0.3 wt%, 6 mg) was added. The hybrid solution was incubated at 37 $^\circ\text{C}$ overnight to yield the hybrid hydrogel.

The sol-gel process is catalyzed by fluoride ions. Here is a proposed mechanism for this process:

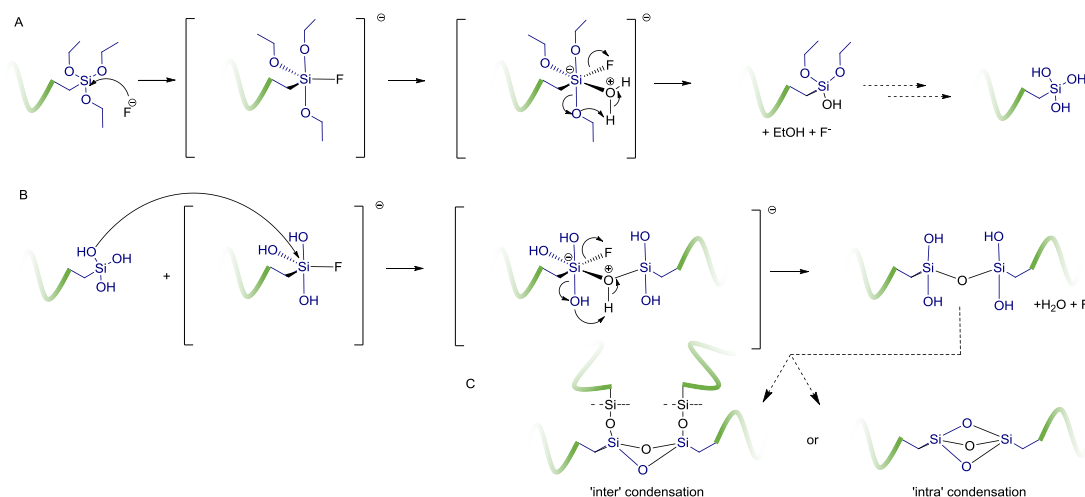


Figure S8. Proposed mechanism for fluoride-catalyzed sol-gel process. A: hydrolysis step. B: condensation step.

NMR study of **2** and monitoring of the gelation process

Preparation of samples

Two NMR samples containing the hybrid peptide **2** (0.062 M) were prepared in similar conditions, one with NaF catalyst and the other one without. The NaF-free sample was used to characterize the undecapeptide **2** in monomeric state since hydrolysis and condensation rates are very low in the absence of NaF. Gelation kinetics were then monitored using the NaF-containing solution.

Hybrid peptide **2** (20 mg, 0.0124 mmol) was dissolved in 200 μL of the following mixture: DPBS \times 10 (Gibco ref 14200, 100 μL), D₂O (100 μL), milliQ H₂O (800 μL), with or without NaF (3 mg). Microtubes were then used to record all spectra on a Bruker Avance 600 AVANCE III spectrometer equipped with a 5 mm quadruple-resonance probe (¹H, ¹³C, ¹⁵N, ³¹P).

Characterization of the compound **2** at the monomeric state (NaF-free sample)

1D ¹H NMR spectra of compound **2** at 62 mM and 0.62 mM were first recorded to check the absence of self-assembly of this short sequence. Then, homonuclear 2D-spectra COSY, TOCSY (DIPS12) and ROESY were typically recorded in the phase-sensitive mode using the States-TPPI method as data matrices of 400 real (t_1) \times 2048 (t_2) complex data points; 4-32 scans per t_1 increment with 1.0 s recovery delay and spectral width of 6009 Hz in both dimensions were used. The mixing times were 80 ms for TOCSY and 300 ms for the ROESY experiments. Spectra were processed with Topspin (Bruker Biospin) and visualized with Topspin or NMRView (B. A. Johnson, R. A. Blevins, *J. Biomol. NMR*, 1994, **4**, 603-614) on a Linux station. The matrices were zero-filled to 1024 (t_1) \times 2048 (t_2) points after apodization by shifted sine-square multiplication and linear prediction in the F1

domain. Chemical shifts were referenced to the trimethylsilylpropanoic acid (TMSP). ^1H chemical shifts were assigned according to classical procedures (K. Wüthrich, *NMR of Proteins and Nucleic acids*; Wiley-Interscience: New York, 1986). The stereochemical assignment of proline and hydroxyproline geminal protons have been performed using the NOE correlations relative to the α protons on the ROESY spectrum. The absence of polymerization of **2** was confirmed performing 1D spectra at different times.

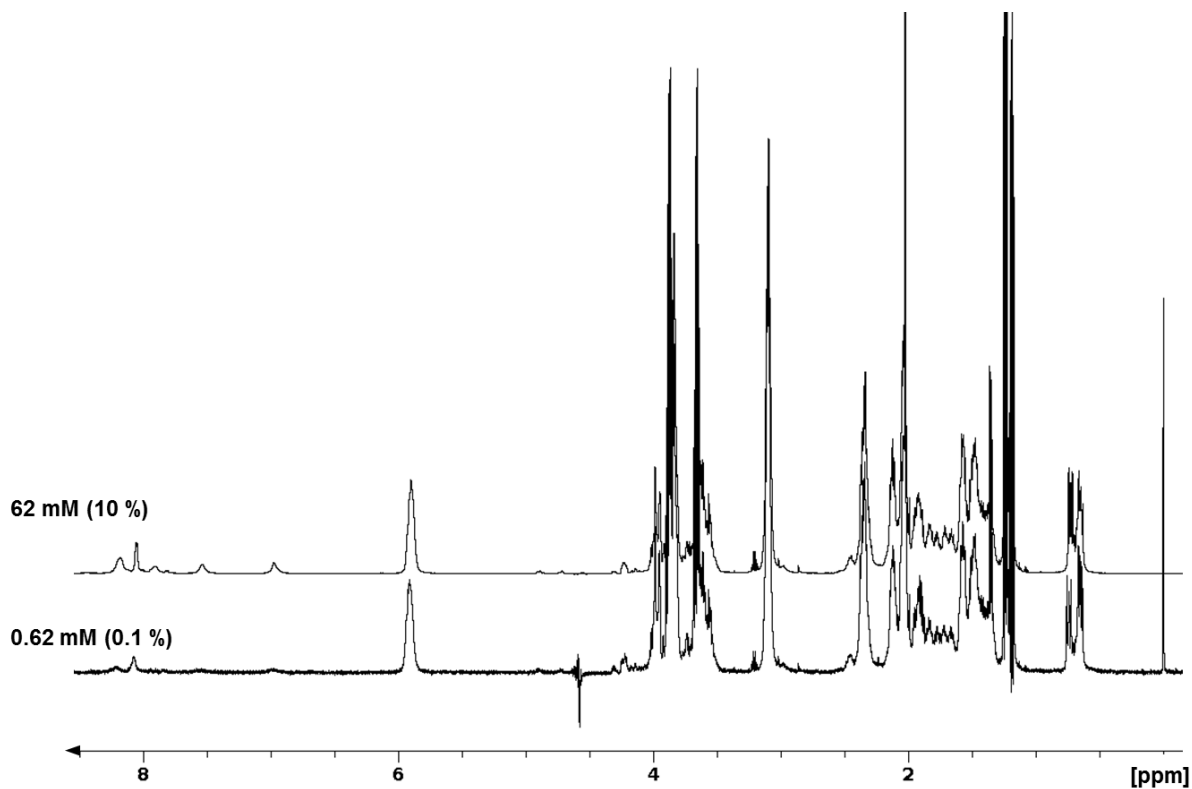


Figure S9. 1D ^1H NMR spectra of the hybrid peptide **2** at 62 mM and 0.62 mM (10 and 0.1%) in DPBS buffer (10% D_2O) without NaF at 37°C, pH 7.2.

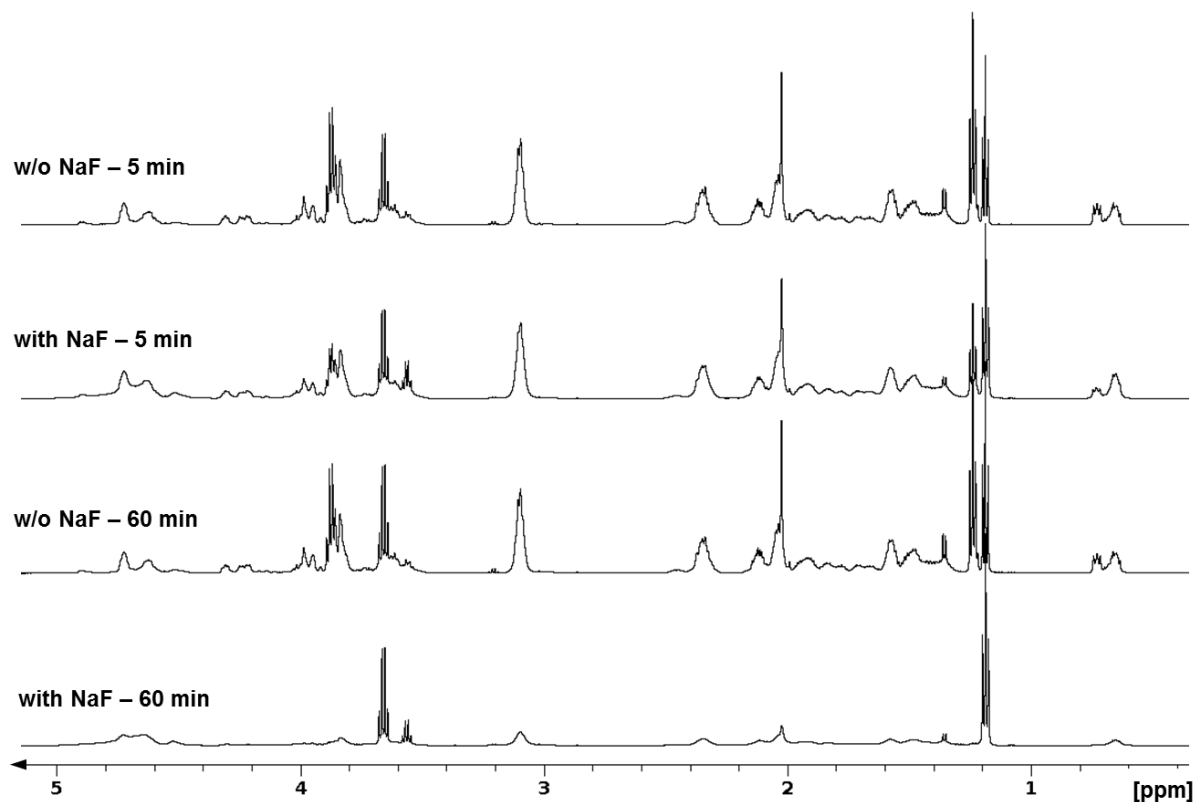


Figure S10. 1D ^1H NMR spectra of the hybrid peptide **2** at 62 mM (10%) in DPBS buffer (10% D_2O) with and without NaF at 37°C , pH 7.2. Spectra were recorded after 5 and 60 min.

Table S1. ^1H NMR chemical shifts of the peptide moieties of the compound **2** in DPBS buffer (10% D_2O), pH 7.2 at 10°C .

Residue	H_N	H_α	H_β	H_γ	H_δ	Others
Lys 1	8.44	4.55	1.68, 1.80	1.46	1.51	H_ϵ 3.13; NH_ϵ 6.12; Ac 2.04
Pro 2	-	4.77	2.35, 1.92	2.06	3.91, 3.65	
Hyp 3	-	4.61	2.39, 2.11	4.66	3.90, 3.85	
Gly 4	8.59	3.98	-	-	-	
Pro 5	-	4.77	2.35, 1.92	2.06	3.61, 3.58	
Hyp 6	-	4.61	2.39, 2.11	4.66	3.90, 3.85	
Gly 7	8.59	3.99	-	-	-	
Pro 8	-	4.77	2.35, 1.92	2.06	3.69	
Hyp 9	-	4.61	2.39, 2.11	4.66	3.90, 3.85	
Gly 10	8.81	3.99	-	-	-	
Lys 11	8.22	4.31	1.74, 1.86	1.39	1.49	H_ϵ 3.11; NH_ϵ 6.12; NH_2 7.25, 7.82

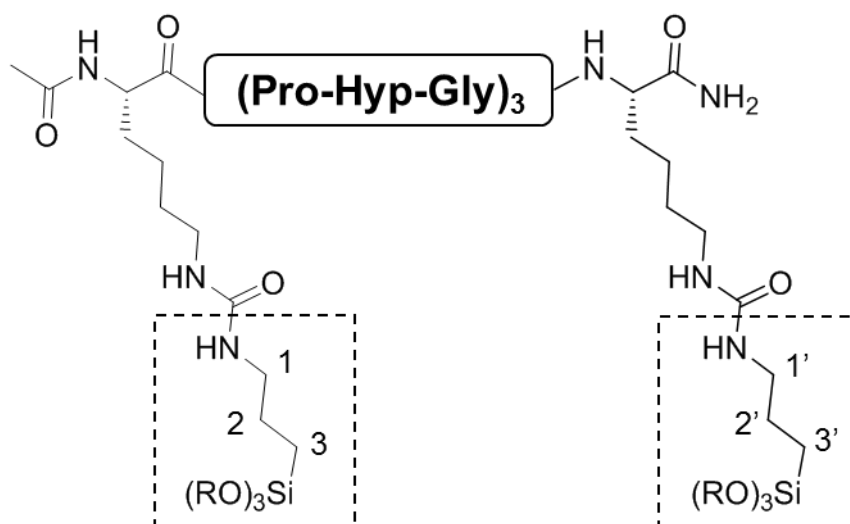


Figure S11. Nomenclature and chemical shifts for the silylated arm (R = -H or -CH₂CH₃)

SiOCH₂CH₃ silylated arm (R = CH₂CH₃): HN = 6.15 ppm; CH₂(1,1') = 3.12 ppm; CH₂(2,2') = 1.58 ppm; CH₂(3,3') = 0.77 ppm; OCH₂CH₃ = 3.90 and 1.24 ppm.

SiOH silylated arm (R = H): HN = 6.12 ppm; CH₂(1') = 3.11 ppm; CH₂(2') = 1.58 ppm; CH₂(3') = 0.66 ppm.

Ethanol NMR signals: CH₂ = 3.67 ppm; CH₃ = 1.18 ppm.

Note: The silylated arm was partially hydrolyzed even in absence of NaF.

Gelation kinetic measurement (NaF-containing sample)

1D ¹H NMR spectra of **2** in DPBS buffer (10 % D₂O) with NaF at pH 7.2 and 37°C were recorded at several intervals (5, 10, 15, 20, 30, 40, 50, 60, 70, 90 and 120 min) to monitor the kinetics of polymerization and gelation of **2**. Spectra were processed and integrals were measured using the Topspin software.

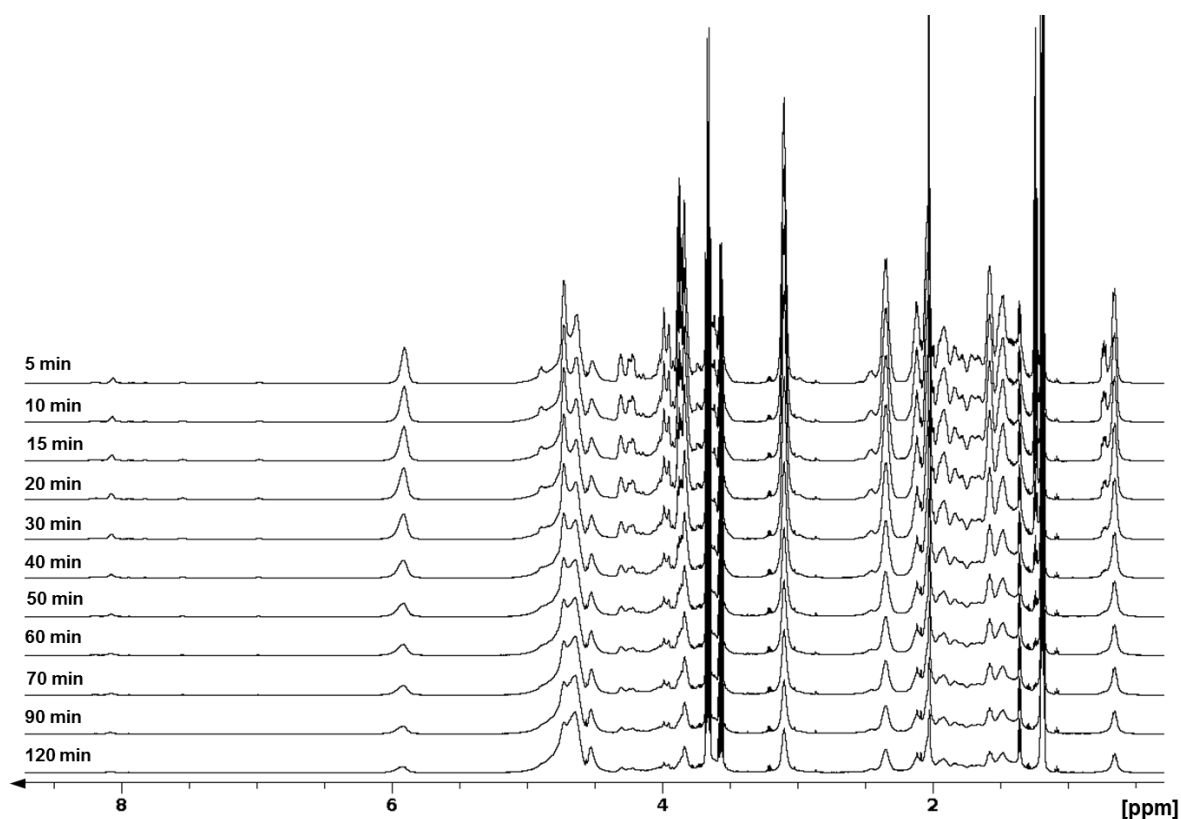


Figure S12. 1D ^1H NMR spectra at different intervals of the hybrid peptide **2** at 62 mM (10%) in DPBS buffer (10% D_2O) with NaF at 37°C, pH 7.2.

CD study

Circular dichroism experiments were carried out using a Jasco J815 spectropolarimeter. The spectra were obtained using a 1 mm path length CD cuvette, at 37°C, over a wavelength range of 190-260 nm. Continuous scanning mode was used, with a response of 1.0 s with 0.2 nm steps and a bandwidth of 2 nm. The signal to noise ratio was improved by acquiring each spectrum over an average of three scans. Baseline was corrected by subtracting the background from the sample spectrum.

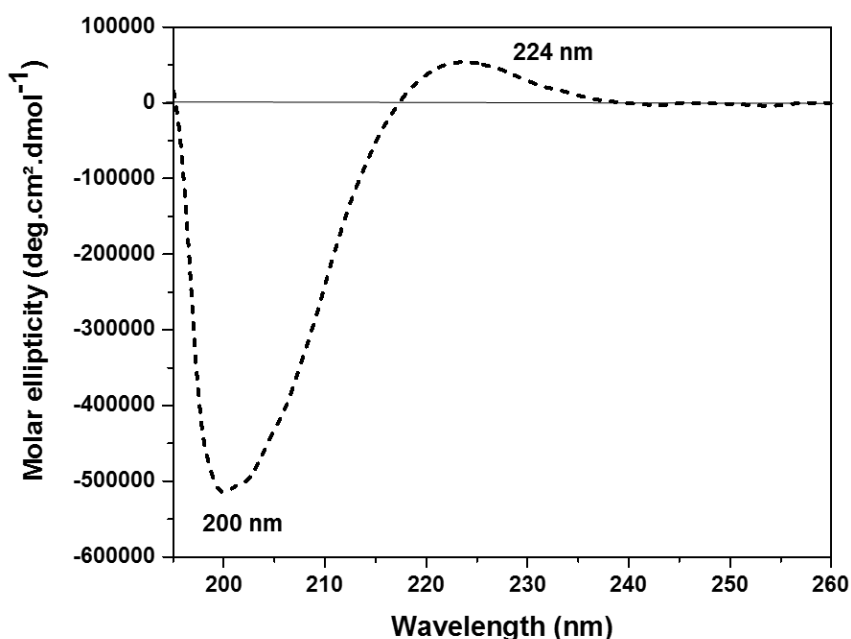


Figure S13. CD spectrum of the hybrid peptide **2** (0.062 mM) in DPBS buffer, pH 7.2 at 37°C.

Rheology

Rheological measurements were carried out on an AR 2000 rheometer from TA instruments, Inc. with a 20 mm diameter parallel geometry at 37°C in the oscillatory mode. The hybrid peptide **2** (50 mg) was dissolved in cell culture medium (10% FBS supplemented DMEM at 37°C, 500 µL) containing sodium fluoride (1.5 mg). The hybrid solution was immediately deposited on the Peltier plate and the gap was set at 500 µm. The excess solution was carefully removed with a pipette and a thin layer of silicone oil was applied to the air/sample interface to prevent dehydration of the sample. After 1 minute equilibration, storage (G') and loss (G'') moduli were recorded as a function of time for 5 hours within the linear viscoelastic regime at 25% strain and 1 Hz frequency. Frequency sweep experiment was also carried out at 25% strain.

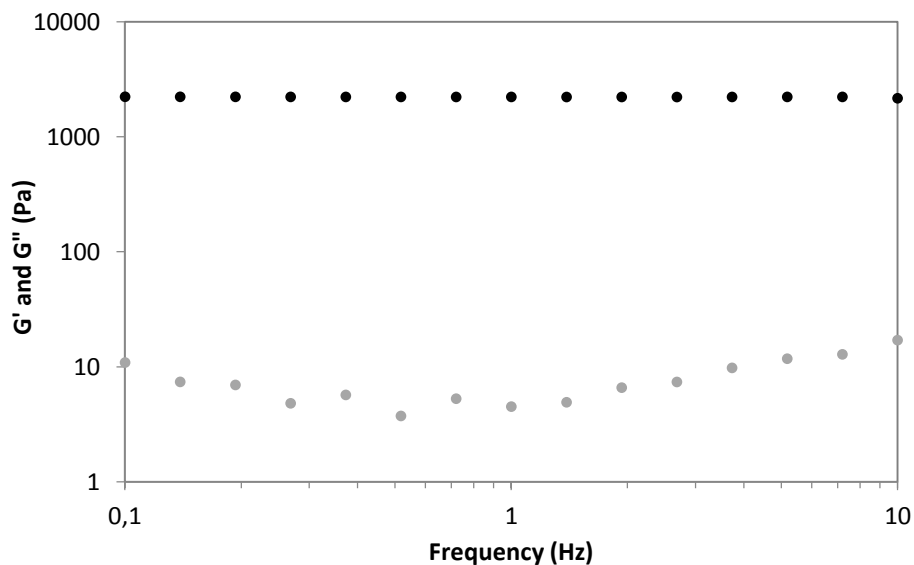


Figure S14. Frequency sweep from 10 to 0.1 Hz at 25% strain. Black dots: G' ; Grey dots: G'' .

Scanning Electron Microscopy

On the one hand, the morphology of the hydrogels was analyzed by Scanning Electron Microscopy (SEM) on a Hitachi S4800. Pieces of gels were affixed to SEM pucks using conductive carbon tape, they were freeze-dried and coated with a 2 nm gold layer.

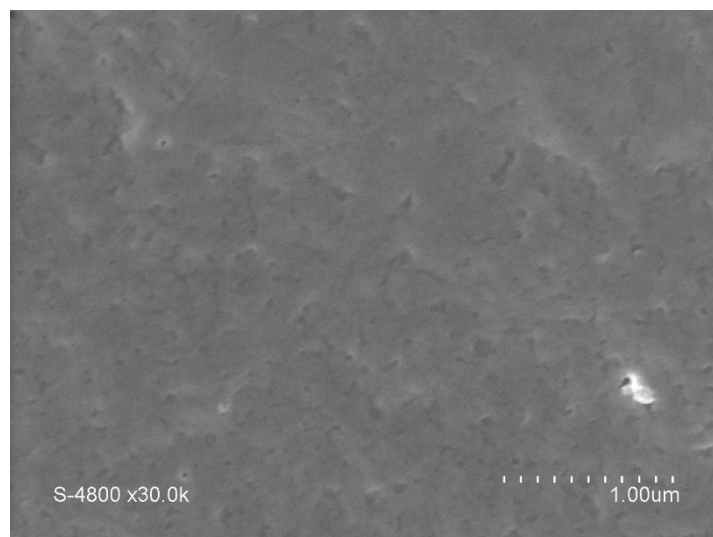
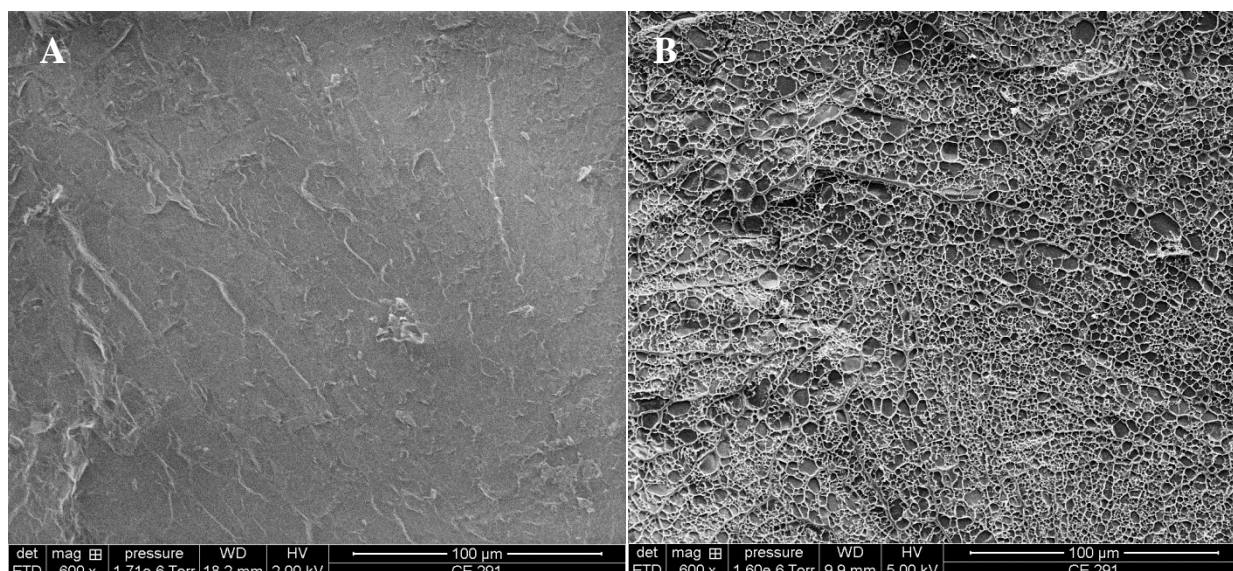


Figure S15. SEM image of a hydrogel (10 wt% of hybrid peptide 2 in DPBS with 0.3 wt% NaF) after freeze-drying

On the other hand, a 10 wt% hybrid peptide 2 hydrogel in cell culture medium was examined by cryo-SEM. The sample was frozen in slush nitrogen, fractured, sublimated for 1 minute at -96°C or 3 minutes at -87°C , coated with Palladium and analyzed at 5KV and -140°C on a FEI Quanta 250 SEM equipped with a Alto 2500 cryo-transfer system (GATAN).



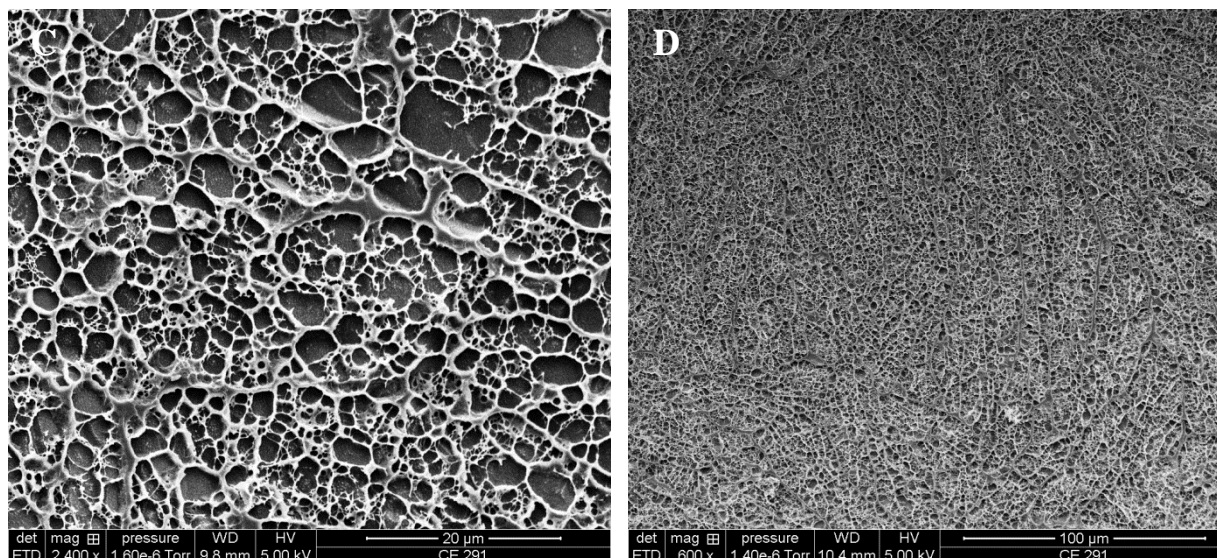


Figure S16. Cryo-SEM images of the hydrogel. A: before sublimation. B and C: after sublimation for 1 min at -96°C . D: after sublimation for 3 min at -87°C .

Cell adhesion

Cell culture reagents were purchased from Gibco and Sigma-Aldrich. Mouse mesenchymal stem cells (mMSC) from Black 6 mice were cultured in high glucose DMEM containing phenol red and GlutaMAX (Gibco ref. 31966) with 10% FBS and 1% penicillin-streptomycin at 37°C with a humidified 5% CO_2 atmosphere. All the assays were run in tetraplicates.

A 10 wt% hybrid peptide **2** solution in cell culture medium was prepared according to the protocol described above. After sterile-filtration, $30\ \mu\text{L}$ of this solution were deposited in wells of a 96 well cell culture plate (flat bottom, TC-PS). A tetraplicate set was prepared for each adhesion time. The plate was incubated at 37°C overnight. The resulting hydrogels were washed with cell culture medium ($3 \times 200\ \mu\text{L}$) before cell seeding. In parallel, collagen foams (ACE surgical supply co, ref DWFN14J1) were cut into discs of 6 mm in diameter, placed in the cell culture plate and washed with cell culture medium ($3 \times 200\ \mu\text{L}$).

Cells (passage n^o23) were detached with trypsin (Trypsine-EDTA solution 0.25%) after washing with DPBS without calcium and magnesium. They were centrifugated, suspended in culture medium and counted with a hemacytometer. The suspension was diluted to a concentration of 60,000 cells per mL. Cells were seeded in the tissue culture treated 96 well cell culture plate, on the hydrogels and on the foams (3 000 cells per well, $50\ \mu\text{L}$). The plate was incubated at 37°C . Cells were allowed to adhere for 30 min, 1h, 2h or 4h at 37°C . Then cell culture medium was removed, wells were washed with DPBS and $50\ \mu\text{L}$ of cell culture medium was added to each well. Only one set of samples was left intact after cell seeding to provide the value corresponding to 100% adhesion. Background wells contained only $50\ \mu\text{L}$ of cell culture medium (no cells). $50\ \mu\text{L}$ of CellTiter-Glo reagent (Promega) was added to each well. The plate was allowed to incubate at room temperature for 8 minutes. Then $50\ \mu\text{L}$ of each sample were transferred to a 96 well opaque white plate for luminescence reading (1 second per well). Background luminescence was subtracted from the obtained values and the results were presented as adherent cell percentage.

Cell proliferation

Cell proliferation on hybrid hydrogels were evaluated on mMSC cultured in the same conditions as for cell adhesion assays. Hydrogels and foam controls were also prepared according to the protocol described in the cell adhesion section. A cell suspension at a concentration of 20,000 cells per mL was prepared (passage n°20). 1 000 cells (50 μ L) were seeded in each well. On the first day, 50 μ L of CellTiter-Glo reagent were added to a set of samples (no prior washing). After incubation (8 minutes at RT), 50 μ L of each well was transferred to a 96 well opaque white plate and luminescence was recorded (1 second per well). 150 μ L of cell culture medium were added to the other sets of samples and the plates were allowed to incubate at 37°C. Each following day, culture medium was removed from a set of samples and replaced by 50 μ L of fresh medium. Cell proliferation was measured out with the CellTiter-Glo assay (50 μ L of the reagent) as previously detailed. Background luminescence was subtracted from the sample luminescence values. Besides, each day, a fresh suspension of cells was prepared, dispensed in a 96 well cell culture plate (50 μ L per well) and subjected to the CellTiter-Glo assay in order to measure the luminescence signal of known number of cells. This signal was used to normalize the sample signals and thus obtain the number of cells.

Encapsulation

The hybrid peptide **2** (30 mg) was dissolved in DMEM (150 μ L) at a 20 wt% concentration. NaF (0.3 mg/mL in DMEM, 100 μ L) was added. The resulting solution was incubated at 37°C for 17.3 hours until its viscosity got high enough to prevent cell sedimentation. 50 μ L of a suspension of mMSC in DMEM (passage n°27, 500 000 cells per mL) were added to the viscous hybrid solution. After homogenization, this solution was dispensed in a TC-PS 96 well plate (30 μ L per well). At the same time, 50 μ L of the same suspension of mMSC in DMEM were diluted with 250 μ L of DMEM to reach the same final cell concentration as in the hybrid solution. 30 μ L of this solution were also dispensed in the TC-PS 96 well plate, these wells were used as controls. The plate was incubated at 37°C for 25h. Then, 100 μ L of the live/dead cell staining solution (PromoKine live/dead cell staining kit II, 0.8 μ L of calcein-AM + 3.2 μ L of EthD-III in 1.6 mL of DPBS) were added on top of the gels and in the control wells. The plate was allowed to incubate at RT for 30 min and hydrogels were examined by laser confocal microscopy on a Leica Sp5-II microscope using the excitation and emission wavelengths recommended by the live/dead cell staining kit supplier. Images were recorded with a 15 μ m pitch in z and were visualized with ImageJ.